2013

Static Structural Implications of Bridge Pile Bents by Vessel Impact under Scoured Conditions

Kakit Fung

THE FLORIDA STATE UNIVERSITY

FAMU-FSU COLLEGE OF ENGINEERING

STATIC STRUCTURAL IMPLICATIONS OF BRIDGE PILE BENTS BY VESSEL IMPACT UNDER SCOURED CONDITIONS

By

KAKIT FUNG

A Thesis submitted to the
Department of Civil & Environmental Engineering
in partial fulfillment of the
requirements for the degree of
Master of Science

Degree Awarded:
Spring Semester, 2013

Kakit Fung defended this thesis on March 29, 2013.

The members of the supervisory committee were:

John Sobanjo

Professor Directing Thesis

Kamal Tawfiq

Committee Member

Sungmoon Jung

Committee Member

The Graduate School has verified and approved the above-named committee members, and certifies that the thesis has been approved in accordance with university requirements.

I dedicate this thesis to the people who all helped make this possible.

ACKNOWLEDGEMENTS

I am grateful to have the opportunity to acknowledge all those who have assisted, guided, and supported me in my studies leading to the completion this thesis. Firstly, I would like to express my special thanks to Dr. Sobanjo for his unwavering support and guidance throughout my studies at Florida State University.

I would also like to thank my committee members Dr. Kamal Tawfiq and Dr. Sungmoon Jung for their invaluable insight and expertise and also extend my sincere appreciation to my family, especially my parents, for their constant support not only for my study at FSU but throughout my entire life.

TABLE OF CONTENTS

LIST OF TABLES

LIST OF FIGURES

ABSTRACT

Local scour has been a leading cause of bridge failure. The erosion of the soil at the bottom of the piles causes changes in the structural integrity of the bridge. Bridge piles are most vulnerable during the occurrence of scour and the process of the scour holes refilling. Outside forces such as vessel impact can occur and cause failure at that time. This solidifies the reason for providing insight on the structural implications of vessel impact on bridge substructures under scoured conditions in hopes that failure can be prevented.

This research involves using FB-Multipier; a nonlinear finite element based program to analyze bridge pile bent induced with impact forces under scoured conditions. The first part of the research deals with exploring the working condition of pile bent under normal flood and scour conditions. The second part deals with the addition of vessel impact striking the substructure. The occurrence of these two conditions occurs under the assumption of an extreme load event occurring.

The changes monitored in the piles were as follows: lateral resistance in the piles when scour occurs; demand/capacity; their fixity based on scour depth; and pile-load interaction. The parameters such as soil properties, bent dimensions, and hydraulic data are modeled after the Ernest Lyons West Island Access Bridge in Florida. This provides actual data that can be used as considerations for similar bridges.

The results mimic the expectations established in the hypothesis. Besides this, interaction behavior of the applied force and piles are found. First off, the location of the applied lateral force is important. It greatly influences the static changes. Maximum shear occurs at the top of the soil during the unscoured and scoured conditions. Maximum negative moment does indeed occur at the fixity depth.

CHAPTER ONE

INTRODUCTION

1.1 Bridge Scour

Scour is the displacement of sediment near the foundation of bridge piers and piers caused by rapid flow or flow strong enough to overcome the shear force of the sediment. It is one of the major causes of bridge failure all around the world with an estimate of 95% of damaged and failed bridges over water bodies are caused by scour (McCann et al. 1999). According to (Lagasse 2013), scour is responsible for 60% of all bridge failures. Scour can be distinguished as Local or Contraction scour. Local scour is further distinguished as Clearwater scour and Live-bed scour. Furthermore, besides this categorization, there are also short-term and long-term scour. The addition of long-term degradation and short-term scour equals total scour. Needless to say, there are other scour types (FHWA 2012) but only local scour in terms of long-term and short-term are considered in this research.

Clearwater by definition is the scour where sediments are not present in the flow. Live-bed on the other hand is the opposite. It is caused when sediment from upstream is carried with the flow and can refill scour holes with less dense soil material. One major deciding factor in local scour resulting in either Clearwater or Live-bed scour is the critical flow velocity. During flood events, low critical velocities tend to induce Clearwater and higher critical velocities tend to induce Live-bed Scour. In other words, if the flow velocity is less than the sediment critical velocity, then Clearwater scour will occur. If the flow velocity is larger than the sediment critical velocity then Live-bed scour will occur.

Long term scour is important because it is involved in determining vessel collision load as previously mentioned. By definition, long term scour tend to occur over a really time period and may be the natural degradation of the riverbed. Just like short term scour many factors can affect long term scour. Unlike short term scour, prediction of long term scour involves more field work like gathering geography information both qualitatively and quantitatively, and physical or

computerized models of an entire geographic area. Fortunately, the bridge plans for West Island Access Bridge provide the long term scour for the vicinity of all the interior pile bents.

Short term scour as the name implies, is scour that occur over a shorter time period than long term scour. It is the scour depths that are developed during storm events. It includes Contraction scour and Local scour. In terms of short term scour, only local scour is considered since the research is focused on separate bridge pile bents. The short term storm scour depth given in the bridge plans are for a 100-year and 500-year storms. Only the 100-year storm event will be considered which is explained in later sections.

Determining scour is a rather complicated process and involves many factors such as water flow velocity, water flow depth, substructure geometry, waterway bed material, and sometimes debris carried by the flow from upstream.

1.2 Scour Measurement

Besides the importance of failure prevention, cost is also important, over design can result in a lot of money wasted. Therefore, accurate scour prediction leads to safe and cost effective designed bridges. Computational methods based on experiments take into account different parameters such as flow, velocity, water depth, and Froude numbers to give approximate values (Coskun 1995) but are not accurate enough. This is leads to experimental methods.

Conventional methods such as borehole core samples and sediment sample collection are very expensive, time-consuming, and not adequate enough to give an accurate prediction. Much extensive research has been carried in search of a perfect means of bridge scour prediction. One particular method is using sonar equipment carried out at the University of Florida. It involves using multiple transducer arrays (MTA) to measure scour depths under different flow conditions (Sheppard 2003). This provides data on the depth of the scour produced but knowledge of sub-riverbed sediment is needed to provide a better understand on minimizing scour.

One such method is the Ground Penetrating Radar (GPR) which is effective in determining the geological structure up to approximately 30 m below the sediment bed (McCann et al. 1999). It utilizes radio electromagnetic waves as opposed to sound waves used in

Sheppard's experiments which is only limited to 5 m and acquisition of data at only one point. Procedure wise, they both are similar in that both types of equipment require sending waves and receiving response, and transferring data to mapping software (Deng and Cai 2010). The GPR is extremely helpful when the scour displacement has been refilled with other sediments and the equilibrium scour depth needs to be known. However, it does come with disadvantages, one is that it cannot be used in waters with high salinity due to complex interaction between electromagnetic waves and saline water that prevents accurate readings, and thus is only effective in freshwater environments (McCann et al. 1999).

The main proposed method of scour measurement in this project is using sonar equipment but knowledge of other methods provides a better look at scour measurement in general. Another apparatus is the "Sedimetri" which are two sensors mounted on a rod that establish a signal when sediment comes between them and proves to be reliable due to not having any moving parts. A series of tests have been carried out on a railroad bridge in Italy using this technology along with sonar equipment. Based on the sonar results, discrepancies can occur during the flood duration. The presence of air bubbles in the water due to violent wave turbulence can act as sonar reflectors which will throw off the readings. Another issue is the presence of larger sand particles suspended above the sediment bed (Mele 2002).

Advanced usage of sonar monitoring of scour is evident at the Indian River inlet in Delaware where a near real-time scour monitoring system is in place that can wake from hibernation and start capturing data at the presence of a design storm. It is advance in that it is possible of 3 Dimensional (Shin 2010) measurement up 100 m in radius due to the capabilities of the 3^{o} cone transducers that can move 180^{o} tilting and 360^{o} circular under precision moving machinery (Puleo 2011). As mentioned before (Mele 2002),the presence of larger sand particles suspended in mid-water leads to less than accurate readings using sonar but using the advanced sonar system (Marine Electronics Ltd.) that utilizes 250kHz transducers improves performance in water bodies with high turbidity (Puleo 2011). Another example is presented in (AASHTO 1997a) describing the heavy suspended sediment in the Yellow River that gives inaccurate readings.

Also, another alternative to sonar is the magnetic sliding collar system. The system works by having steel rods driven into the sediment bed and the sliding collar will continue to drop as scour occurs (AASHTO 1997b). One downside is that the collar will not show any indication that the scour hole has been filled with foreign sediment once the maximum scour depth has been reached. The National Cooperative Highway Research Program (NCHRP) has conducted research on different fixed instrumentations for measuring scour and has decided on the two likely alternative; sonic fathometer (sonar) and magnetic sliding collar as mentioned above (AASHTO 1997b). They are chosen based on factors such as type, cost, maintenance, installation, etc. From the continued research and experiments, data on both systems have been compiled into two separate reports; Sonar Scour Monitor Report 397A and Magnetic Sliding Collar Scour Monitor Report 397B.

A further look at the sonar system shows that despite the system is useful in monitoring scour; there are still unknown factors that come into play. Factors such as water temperature, submerged water depth or environmental conditions can or cannot alter the readings. For example, the depth is calculated from the travel time the pulse takes due to the speed of sound in water being constant but the variable of speed is depended on density which in turn is depended on temperature (AASHTO 1997c). One of the challenges is to find the differences by performing field experiments indoor and outdoor.

1.3 Structural Implications

There are many countermeasures to protect against scour at piers and abutments, but sometimes these protections aren't enough because they can likely fail under certain circumstances. One example would be riprap. According to (Unger and Hager 2006), riprap can fail due to overwhelming shear force or undermining under the riprap. In order to properly protect against failure due to scour, the structural implications need to be known when the substructure undergoes scour.

A recent study (Bennett et al. 2012) has been made on using integrated analysis technique to separately model substructure and superstructure and then combine the analyses to form a complete analysis. The results show that an increase in scour depth decreases the shear forces of pile caps at the piers. On the other hand, shear forces and bending moments on the piles will

increase. Overall, deflection of the pile caps will increase and also causes the bridge deck to deflect laterally but bucking of the piles is not an issue (Bennett et al. 2012). Another paper suggests that buckling is an issue when it comes to piles under extreme scoured conditions by using a P-Y Approach to analyze the buckling. The results show that the boundary conditions of the pile clearly affect buckling at smaller scour depths but it is unclear on the results are affected at larger depths. Besides elastic buckling, inelastic buckling of the piers should also be considered (Lin et al. 2012). A list of different boundary conditions for piles is presented in the literature review performed by (Liang 2012). This provides a general idea how piles are evaluated under scoured conditions. Buckling analysis will not be part of the scope for this project.

Besides the static implications scour has on bridge piers, the bridge is also affected dynamically. (Sabia 2011) has conducted experiments on the dynamic response on both before and after retrofitting the bridge for damages caused by scour under different parameters. According to (Wang and Kallaka 2011), several effects can occur due to scour. First the hydrodynamic force can increase significantly which in turn increases the bending moment on the pier. The pier may then fail due to excessive bending moment when a severe flood storm follows the scouring. Second is the effect on the structural stiffness of the pier which in turns affects the natural frequency. Because of the increased height due to scour, the base shear force can increases substantially.

1.4 Vessel Impact

In the United States alone, approximately 2,692 vessel collisions occurred between 1992 and 2001(McVay et al. 2012). Any bridge or bridge component in a waterway with water depths of 2.0ft or deeper accessible by vessels shall be designed for vessel impact according to the LRFD Bridge Specifications (AASHTO). Besides bridge failure due to scour, bridge failure can also occur caused from impact by vessels. According to the Vessel Collision Design of Highway Bridge Specifications, there have been 31 major bridge collapses caused by vessel collision (AASHTO 2009). The causes for vessel impact are numerous and the determination for the occurrence of bridge failure is complicated and involves different factors. The causes for an

errant vessel are also rather complicated and thus the overall process of the design and evaluating new and existing bridges is a complicated matter.

The AASHTO Bridge Specification describes three methods for determining design vessels for different components of a bridge structure. The first method (Method I) is a semi-deterministic procedure, the second method (Method II) is a more detailed risk analysis, and the third method (Method III) is a cost-effective approach for risk reduction (AASHTO). Particular the Vessel Collision Design of Highway Bridges Specification focuses on the second method unless otherwise noted (AASHTO 2009). New bridges shall conform to this specification. Existing bridges over waterways with commercial vessel traffic are evaluated using the second method to determine their vulnerability and proper actions are taken to reduce their vulnerability. According to the FDOT Drainage Manual, pile bents subjected to minor vessel are to be designed to remain structurally adequate even when one pile is damaged and removed.

The main focus of vessel impact in this research is to assess the result of including design vessels hitting the bridge substructure under scoured conditions. Instead of using Method II to determine the probability of failure just through a set of procedures which does not include a scour factor, failure can be assessed through other analytical means. By knowing the structure implications caused by vessel impact, the structure can be strengthened for that particular purpose and thus the chance of failure can be reduced. One important factor to consider is the draft depth of the design vessel. If the draft depth of the vessel is larger than the water depth then there is no possibility that the vessel can strike the pile bent. The draft depth that will be considered is the empty vessel draft depth because the presence of an extreme load event occurrence which is explained in the following section.

1.5 Extreme Load Event

The reason for combining bridge scour and vessel impact contradicts the idea that during heavy storms which induces scour, vessels and barges cease operation and the chance of them occurring is relatively low. In the “Design of Bridges for Extreme Events” conference held by the Federal Highway Administration (FHWA), (Nowak and Knott 1996) recommended two load cases which account for those occurrences.

The first case involves an empty barge loose from its moorings and carried by a heavy storm which can at a higher probability hit the bridge substructure. The impact force is thus determined by the vessel tonnage weight and flow velocity. According to the Vessel Collisions Specifications, the impact load shall be combined with one half of the long-term scour and one half of the short-term scour. The short term portion is the scour associated with the 100-year storm event.

The second case involves maximum impact loads of design vessels hitting the bridge under normal everyday conditions with the addition of one half the long term scour. Depending on the magnitude of the hydrodynamic force in the transverse direction, only the first case will be considered since it is likely the more severe of the two cases. If the hydrodynamic force has high enough magnitude to cause severe damage then it's deemed important to be considered an extreme case. One half of long term scour is just too insignificant to cause high magnitudes of hydrodynamic force. Because of the nature of an extreme event occurring, the likeliness of having vehicular traffic (gravity loads) present is rather small so the effect of gravity loads in the model will be absent.

The AASHTO LRFD Bridge Specifications label this load combination under the "Extreme Event II" which includes everything from vessel collision to check floods. This load combination has a live load reduction but for the simplicity of this research, the presence of live loads such as pedestrians and vehicles will be completely eliminated. For the "Extreme Event II", the load factor for vessel collision is 1.0.

1.6 Hypothesis

The expected results should be able show clear changes in the static changes of the bridge substructure. Since the geometry of the substructure remains the same besides the battered ratio, and the only factor changing is the soil depth and the pile lateral resistance is dependent on the soil depth, the result will likely show a decrease in lateral resistance of the substructure. Besides the decrease in lateral resistance, moment in the piles should increase due to its increasing unbraced length (moment arm). Shear at the base of the piles will likely increase. This will likely happen since laterally loaded piles follow the classic beam theory. The objective is to see how

much change occurs in terms of moment and shear, and the scour depth threshold at which the structure fails.

The end piles are likely the ones providing most of the resistance for the pile bent. The increase battered ratio will likely induced some noticeable changes in how the substructure handles the impact forces. Portion of the force will be resisted axially by the piles.

1.7 Research Objectives

The objectives of this research are to find the structural changes when drifting vessels such as barges break loose from its moorings and strike a bridge substructure during heavy storms that cause excessive scour and find out how the two can affect the bridge substructure in terms of lateral resistance, moment and shear capacities. One such objective is to observe a relationship between the distribution of forces to the piles and the applied lateral load. For the purpose of this research, the substructure of the Ernest Lyons West Island Access Bridge will be investigated. A brief description of the bridge is given in the following chapter. Most of the information needed for this research is provided in the bridge plans whereas some difficult to obtain information will be assumed with good engineering judgment. This research is conducted with the knowledge that not many experiments or research have been conducted in this field, thus the challenge is coming with needed parameters relating to vessel collisions.

CHAPTER TWO

MATERIALS AND METHODS

2.1 Substructure Model

The substructure is modeled as one of the pile bents of the Ernest Lyons West Island Access Bridge. The pile bents support ten 50ft of AASHTO girders. This bridge along with the identical East Island Access supplements the 4600ft long Ernest F. Lyons replacement segmental bridge (Ellis 2008). This bridge is located over the Intracoastal Waterway in Martin County, Florida.

The piles are embedded in a soil profile similar to the soil present at the Ernest Lyons bridge site which is discussed in the next section. The bent consists of 5 standard FDOT 24" squared prestressed concrete piles. This particular pile cross section data is built into the software. The end piles (Pile#1&5) are battered. According to the FDOT, piles not subjected to ship impact should not exceed the maximum slope of 1:12 (horizontal to vertical). For the piles subjected to ship impact, the slope should not exceed 1:4. In this case, the bridge was never designed for vessel impact but the unforeseen events can occur like vessel collision. The increased horizontal to vertical ratio of 1:4 will be assessed.

The pile cap is made up of a 3.25ft x 3.5ft reinforced concrete beam with overhang of 3ft on each side. AASHTO Type II girders sit on top the cap. The minimum pile embedment length into the cap is 1.0 ft. Determination of the connection type is important. According to (Rollins and Stenlund 2010), one foot of embedment developed between 61 and 83% of fixed connection moment and is only considered partially fixed. For this project, a fixed connection will be utilized. This will provide moment values at the pile head. The prestressed piles are spaced at 11ft. The pile cap is 3.25ft in depth. The average bent elevation of all interior pile bents is 15.6ft above ground. That is measure from each pile bent's midpoint. That gives an average pile length of 55.6ft; that includes a minimum tip elevation of 40ft below the top of the soil layer. The following figures show the steel reinforcement of the pile cap, simple illustration of the pile bent, and prestressed pile details respectively (FDOT 2013).

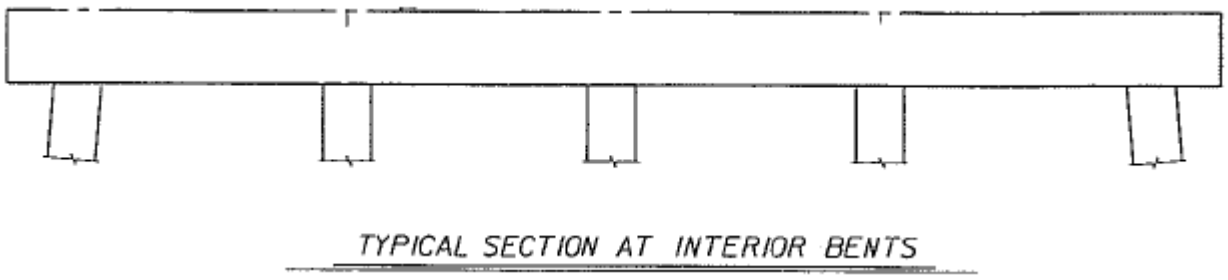

Figure 2.1 Ernest Lyons West Island Access Bridge typical pile bent

Figure 2.1 shows the typical section of the interior bents taken from the bridge plans. Figure 2.2 shows the steel reinforcement of the pile cap with dimensions. This is not a standard pile cap but it is specific for these particular pile bents.

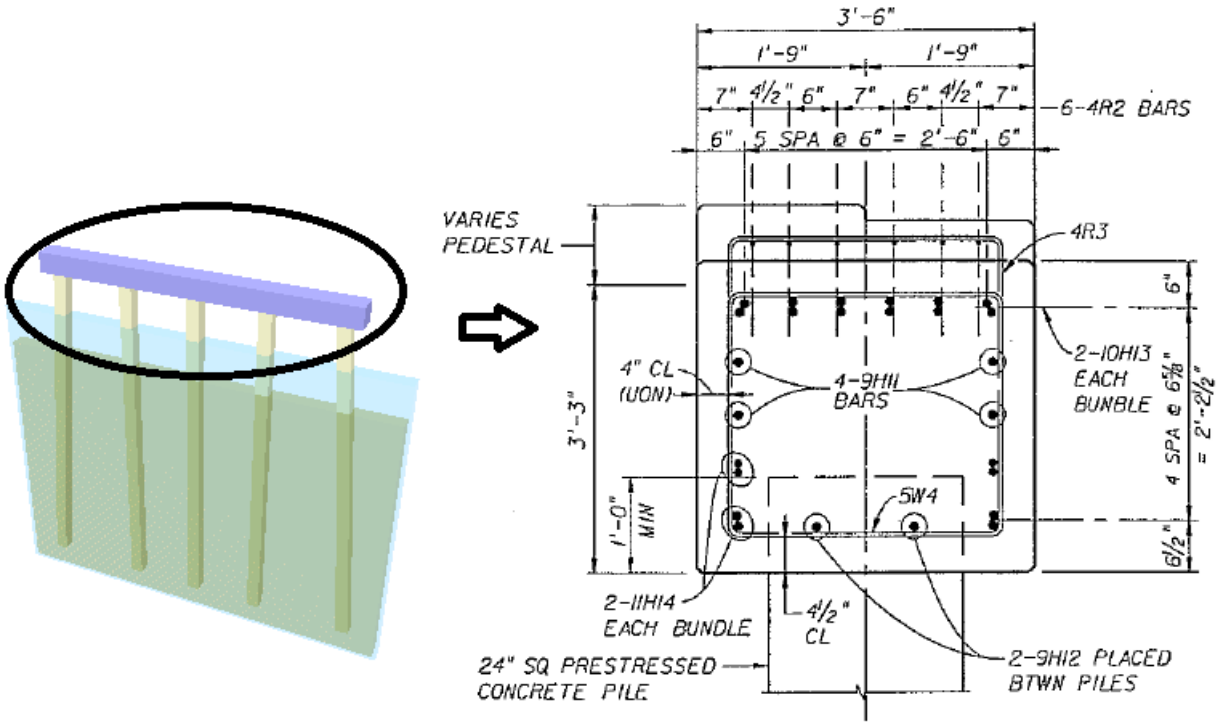

Figure 2.2 Pile cap steel reinforcement diagram

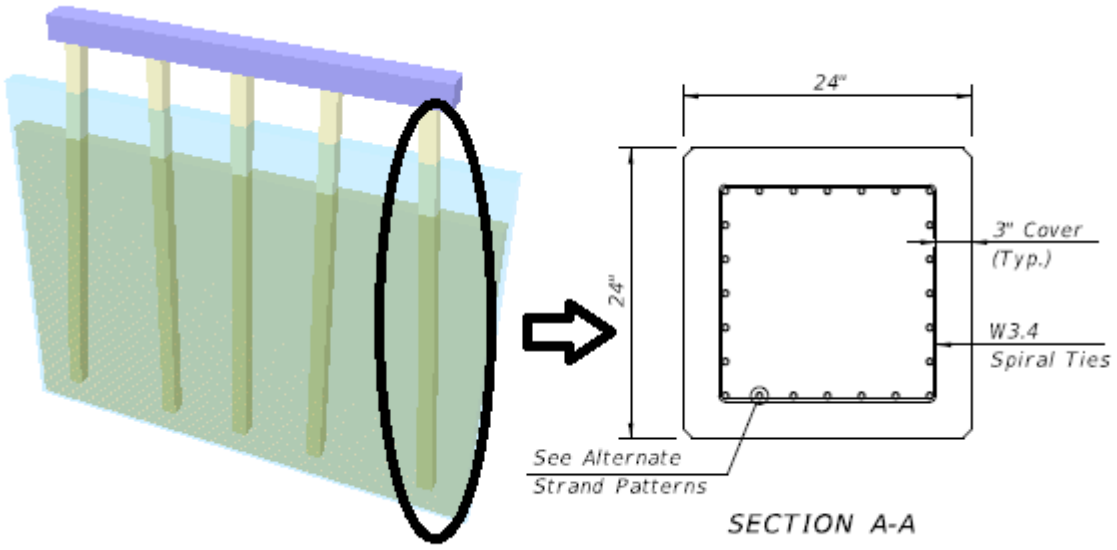

Figure 2.3 Standard 24" sq. FDOT prestressed pile section

Figure 2.3 above shows the general prestressed steel in the pile section. This reinforcement is for the middle portion of the pile. The ends of the piles are reinforced with a different strand patterns. The software has the pile data already built into the system. Figure 2.4 shows the standard 24" squared prestressed reinforcement as a built-in choice in FB-Multipier, same as the one shown in the bridge plans. It is available in the section database or the user can manually input the strand configuration. By choosing the standard 24" squared prestressed pile, the width and depth are automatically specified but the length needs to be input by the user. The top right shows the orientation of axes of the pile. The pile bent can contain several different types of piles but in this case, all piles are the same.

The same procedures are used for the pile cap but since pile cap is not a standard beam, it is not listed in the section database so the user has to manually input the steel reinforcement which is a fairly easy process. The software requires the pile-pile cap embedment length but on the plans, a minimum value of 1ft is shown. It is unknown how much embedment are after construction so a value of 1ft is assumed for piles into pile cap.

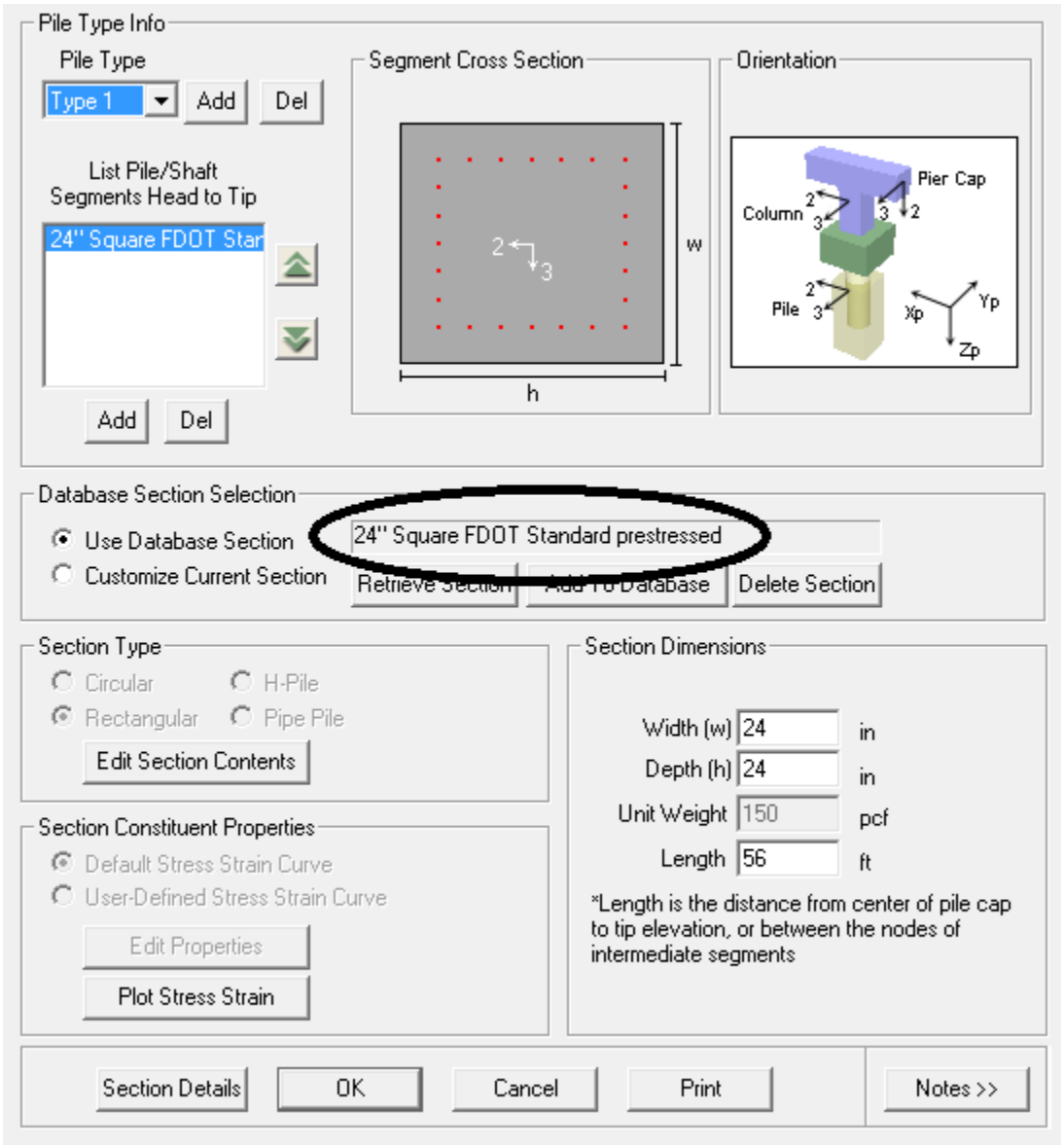

Figure 2.4 FB-Multipier pile information input in FB-Multipier Software

The capacity of the pile is the interaction of axial and bending capacity of the pile. Figure 2.5 shows the pile interaction diagram of the FDOT 24" squared prestressed pile. The same interaction behavior is seen for all the elements within the pile and for every pile which is expected. For pure bending, the pile can resist approximately 600kip-ft.

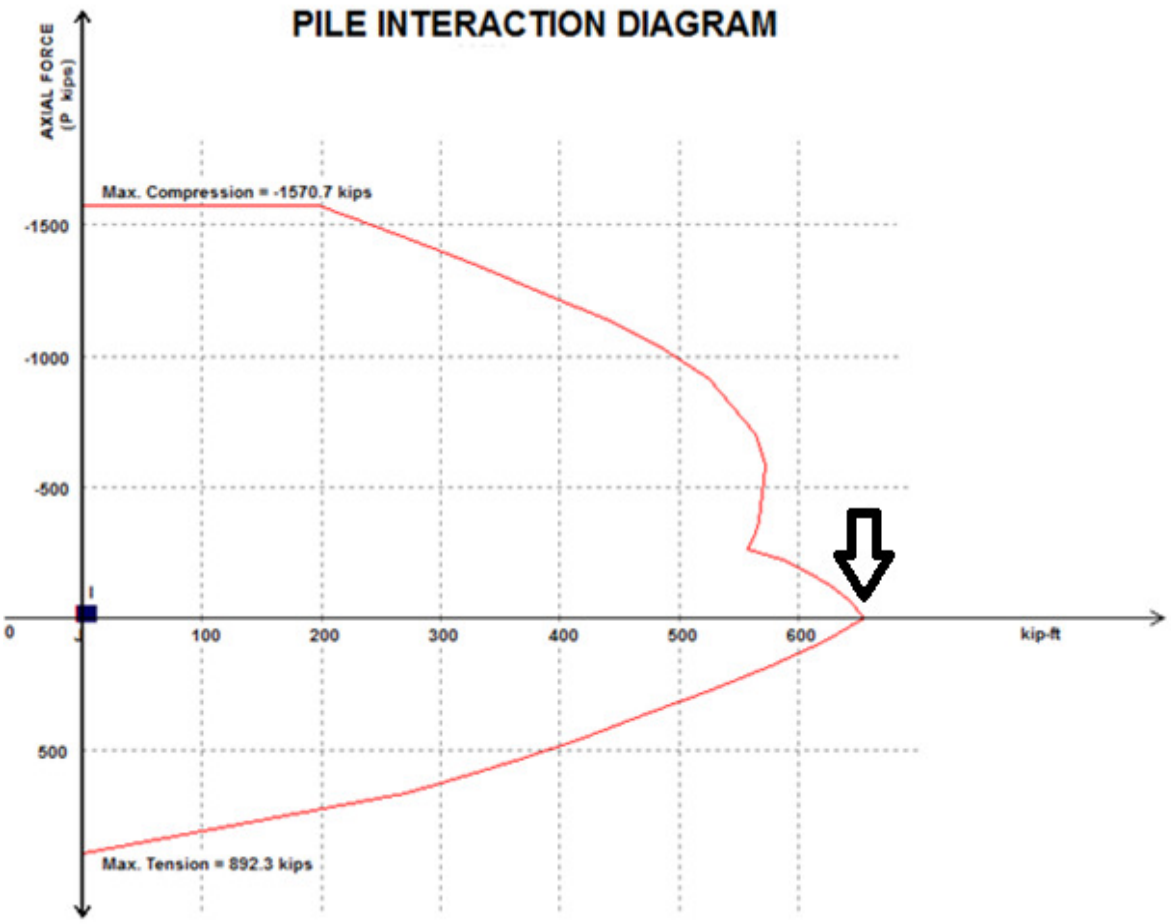

Figure 2.5 Prestressed pile interaction diagram

2.2 Scour Depth

The average long term scour elevation for all ten interior pile bents is given in the bridge plans along with the values for average 100-year scour elevation and 500-year scour elevation for all ten interior pile bents. Since the basis of this research is to know the structural implications of pile bents under scoured conditions, it is important to extend the scour depths beyond the maximum/equilibrium scour depth. That way, the changes can be observed and conclusions can be made for very extreme conditions. For the simplicity of analyzing bridge substructure under scoured conditions, only clearwater scour will be assumed and if live-bed scour does occur then refilled scour holes will be analyzed as though the soil had not refill the

hole. The average maximum 100-year scour elevation for all ten interior pile bents is -10.79ft. The average maximum long-term scour elevation for all ten interior pile bents is -5.94ft below the ground level. The scour depth will start at zero (unscoured) and increase at an increment of a portion of the equilibrium (maximum) scour stated in the bridge plans. The model will also be subjected to additional scour beyond that of the maximum value. That is to investigate the effects of excessive scour and push the substructure to its limits.

2.3 Hydrodynamic Force

According to the AASHTO Vessel Collision guide, short-term scour is associated with the 100-year storm event. The average velocity given in the bridge plans is 4.4ft/s. The model will be first subjected to unscoured hydrodynamic force. The hydrodynamics forces increases as the scour depth increases. So for every run, the hydrodynamic force will be different. The method used to calculate water pressure needed to calculate the hydrodynamic force is taken from chapter 3 of the AASHTO-LFRD Bridge Design Specifications. This equation takes into account the water parameters such as specific weight of water which is a function of other parameters such as temperature and salinity. For vessel impact, in the longitudinal direction, the substructure is subjected to 100% of the impact force; half of the impact force strikes the transverse direction of the piles. The calculated water pressure is a triangular distributed load imposed on the pile. The following shows this equation to calculate the hydrodynamic force in the longitudinal direction:

$$P = C_D \frac{w}{2g} V^2$$

Where P = water pressure (psf)

C_D = drag coefficient (longitudinal direction)

w = specific weight of water ($62.3 lb/ft^3$)

g = gravitational acceleration ($32.2 ft/s^2$)

V = flow velocity (ft/s)

Few things to note are that the specific weight of water can also change slightly due to sediments in the water (live-bed scour) but for the consistency of this research, it shall remain at 62.3lb/ft^3 for all scenarios of scour. In the LRFD Bridge Specifications, a simple table of drag coefficients is provided for different pier/pile geometries. The pile cross section in this research best fits that of a squared-ended pier/pile. That yields a C_D of 1.4 and a C_L of 1.0. The following is the equation for calculating hydrodynamic force in the transverse direction:

$$P = C_L \frac{w}{2g} V^2$$

Where P = water pressure (psf)

C_L = drag coefficient (transverse direction)

w = specific weight of water (62.3lb/ft^3)

g = gravitational acceleration (32.2ft/s^2)

V = flow velocity (ft/s)

$$F_D = \frac{1}{2} P A_e$$

Where F_D = static hydrodynamic force acting on substructure

A_e = effective frontal area where upon the force acts

The resultant static hydrodynamic force is applied at a point that is one third the distance from the top of mean water level due to the triangular nature of the load. One important thing to note is the code states the load to be triangular but in actuality, the hydrodynamic force is more parabolic than triangular thus the calculated force should be slightly less than the actual force and the resultant force should be located lower below the water surface. For the simplicity of this research, the hydrodynamic force is portrayed in the code. Figure 2.6 shows the hydrodynamic force as a triangular distributed load and the relative location of the resultant force. Prematurely, it can be foretold that the force will be very low in magnitude due to the short water depth even with the occurrence of a 100-year storm.

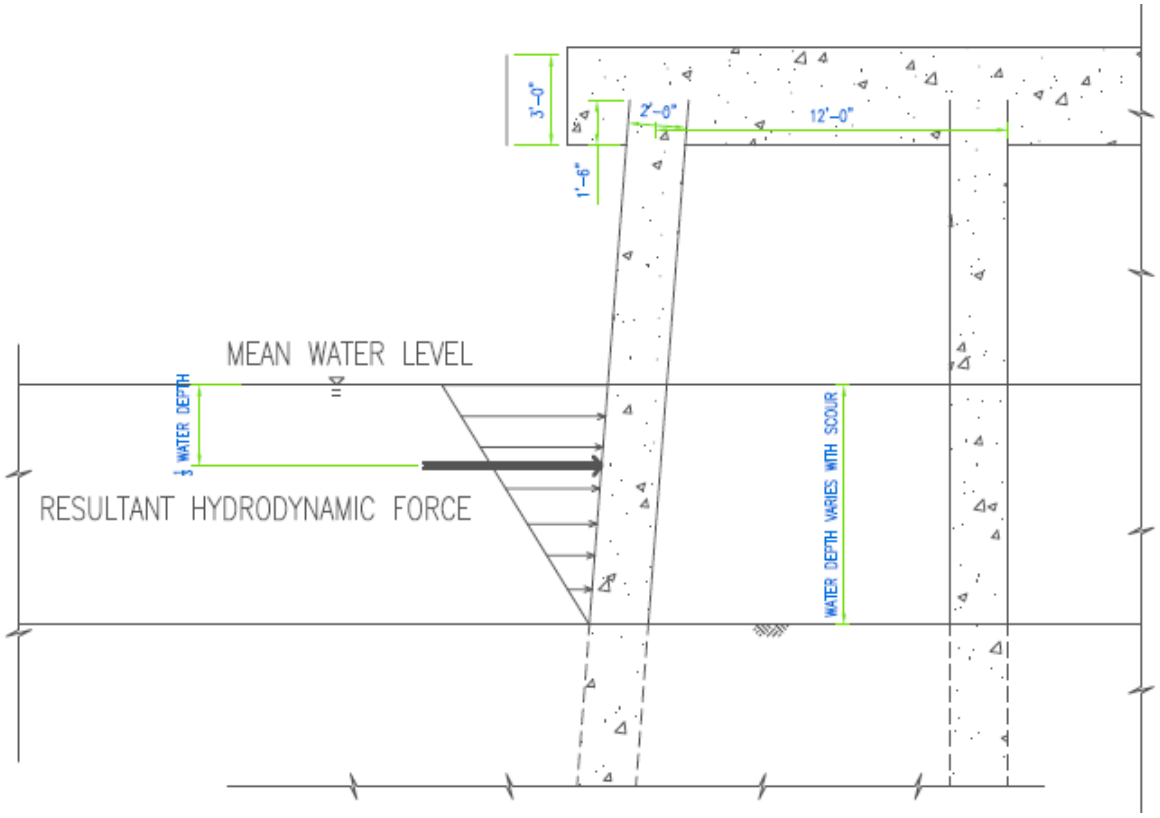

Figure 2.6 Location of resultant hydrodynamic force

Based on the hydraulics data given on the bridges, a value of 8ft is used for the flow depth during the 100-year storm event. That is sum of the average water depth found in the soil borings plus the increase flow depth during the storm event. First off, the hydrodynamic force for unscoured flood condition is determined and that will be the minimum. Then for each increment of one fifth of the sum of half the long-term scour and half of the short-term scour, a new hydrodynamic force is determined. That increment rate should be able to yield a noticeable increase in force.

The percentage of their magnitude compared to that of the impact force is very insignificant. They do not even match 1% of the impact force. It is safe to neglect the hydrodynamic forces completely after the initial run of the model under normal flood conditions. Also, due to the very low magnitude of the hydrodynamic force, only the first extreme event is considered because that is likely the most severe damaging event.

In actuality, the hydrodynamic force will not only strike the longitudinal face of the first pile only but rather strike the longitudinal faces of all the piles as well. This is also true for the traverse direction. The code also states an equation for determining the hydrodynamic force for the transverse direction. For the purpose of keeping this research more focused on the actual structural aspects, this direction will be neglected.

2.4 Vessel Impact Force

AASHTO Vessel Collision Specifications indicate that impact forces are computed equivalent static loads acting upon a substructure. These static loads are determined based on their kinetic energy which is a function of mass and velocity (McVay et al. 2012). Large scale impact research was conducted to assess these forces at different barge velocities. The barge used was 50 ft wide by 150 ft long with a draft of 3 to 10 ft. The velocity (design impact speed) is determined to be the transit speed of the typical vessel traveling in that particular waterway. This design speed shall be less than the minimum design speed which is equal to the yearly mean current for that particular waterway. The mass is the mass of the design vessel striking the pier.

Based on research conducted using large scale testing, an empirical equation was developed to calculate static vessel collision force on the bridge pier. This is recommended by the AASHTO Vessel Collision Specifications Guide.

$$P_s = 220(DWT)^{\frac{1}{2}}\frac{V}{27}$$

Where P_s = static vessel collision force (kips)

DWT = deadweight tonnage of vessel (tones)

V = vessel velocity (ft/s)

The Vessel Collision Guide states that for new substructure designs, the location of the design impact force is applied as an equivalent static load to the impacted area of the substructure parallel to the alignment of the centerline of the channel. From the total static force, 50% of it is applied to the side of the substructure at 90 degrees to the channel centerline. Both situations cannot simultaneously. Depending on the magnitude of the hydrodynamic force, only one impact locations will be looked at in this research to assess the most severe changes in

structural changes. The design impact force is applied as a single concentrated static force on the substructure at the mean water level which means during high flood events, that mean water level is higher than normal. The actual location of the impact will be different due to the geometry limitations. The bow of the barge will likely strike the top of the pile cap. This is illustrated in the following diagram (Figure 2.7).

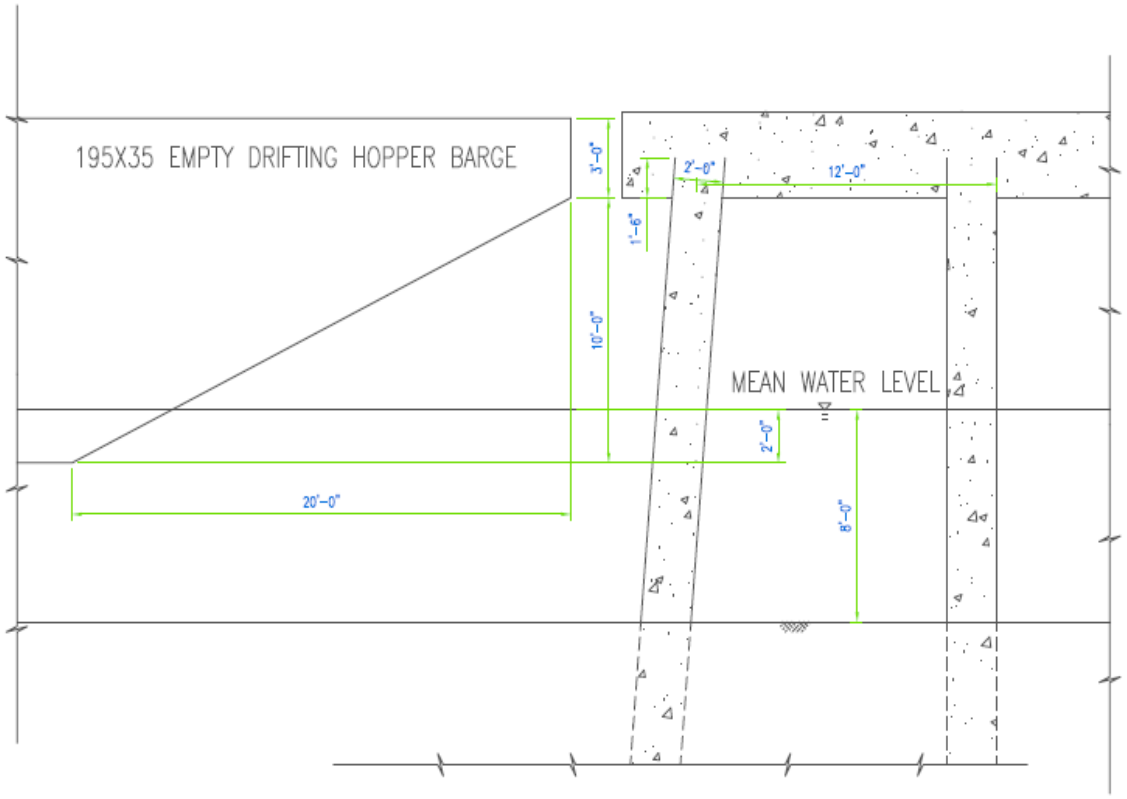

Figure 2.7 Vessel impact diagram

The code states that the design impact speed is determined based on the typical vessel transition speed with that channel. For the simplicity of this research, the vessel design impact speed will be taken as the 100-year flood event flow velocity. According to the Vessel Collision Guide, all bridge substructures shall be subjected to the minimum impact load which is the collision of an empty 195 x 35 drifting hopper barge in the water depths greater than 2.0ft. This

design vessel is the minimum load that is also used in research conducted by (Consolazio 2009) . Since the availability of vessel data is nonexistent for this particular bridge. The minimum design vessel will be used. This barge meets the draft depth and width requirements. It is able to transit between pile bents and strike the piles transversely.

Using the impact equations in previous section with input values of 3.4 ft/s for the average velocity and deadweight tonnage of 252.6 tones, a value of 427.6 kips is calculated. During the initial run of the software, the pile bent can only handle 300 kips of impact force (70%). Values higher than this will cause the substructure to fail. For all the analysis runs, 200kips (50%) of the impact force will be used. This magnitude of impact provides a good balance of scour depth and impact force; having a high magnitude of impact force will diminish the amount of scour depth the pile bent can handle and vice versa.

2.5 Soil Characteristics

Having the correct soil profile in which the piles are embedded in is extremely important since the lateral strength of the piles is provided by the soil. The soil profile is modeled after the soil surrounding the Ernest Lyons West Island Access Bridge. Figure 2.8 below shows the relative location of the borings for the Access Bridge, i.e. W-8, W-10, etc.

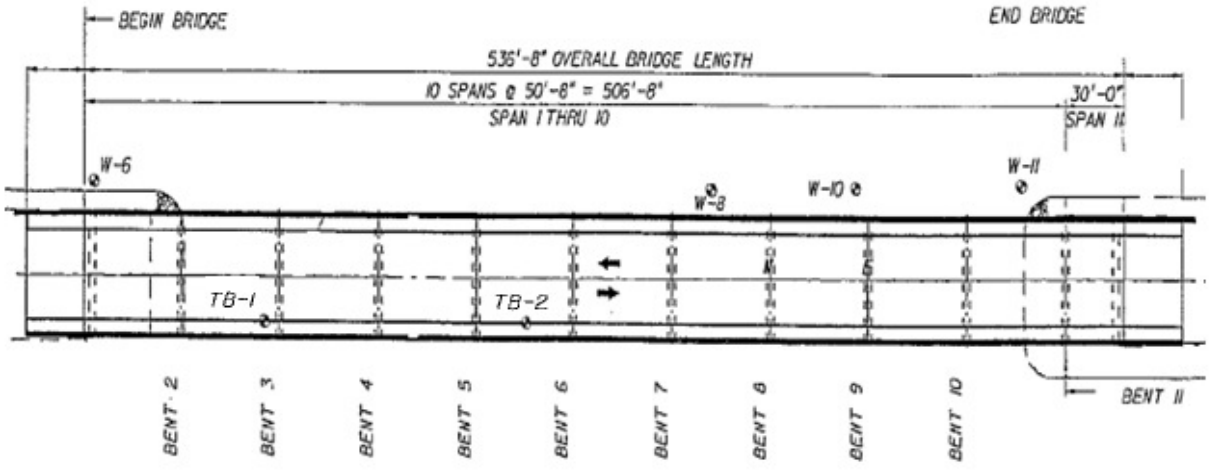

Figure 2.8 Plan view of bridge and relative soil boring locations

The data is taken from the bridge plans. For the purpose of this research, the borings located nearest to the center of the bridge are chosen to represent the soil profile under the assumption that the vessel will strike bents in that vicinity. This barge can also strike the ends of the bridge but there are obstacles like riprap stopping the vessel from striking the exterior pile bents. The "T-1" and "T-2" borings (Figure 2.10) show up to 100ft and "W-8" and "W-10" (Figure 2.9) borings show up to 50ft and 100ft below the mean water level respectively. These borings show relatively similar profiles.

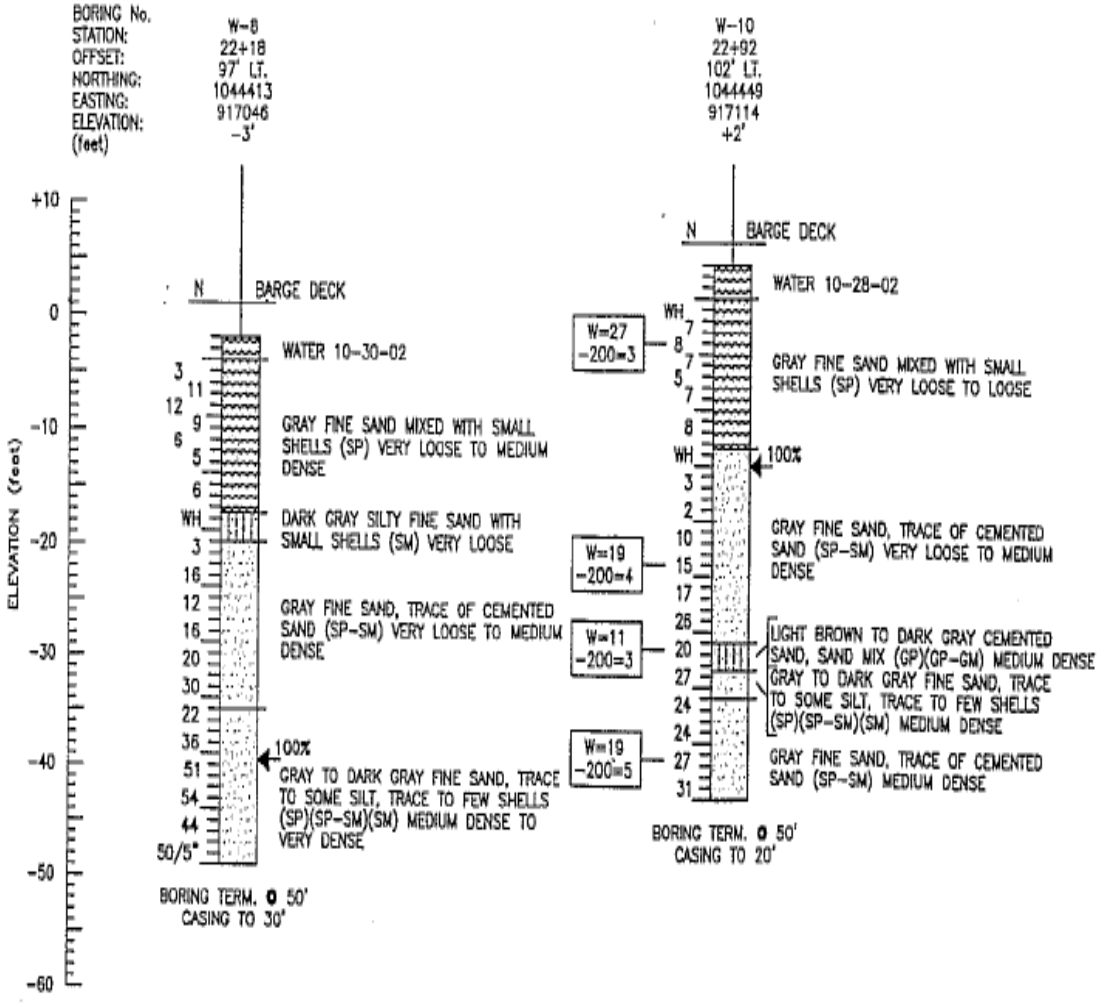

Figure 2.9 Borings "W-8" (left) and "W-10" (right) taken from bridge plans

The type of soil present is sand. The top layer shows an approximate of 7ft of mostly gray fine sand mixed with small shells and other things. This is typical of the shores and beaches. This is particularly true for all first layers in all the borings. The second layer also remains constant for all the borings which is made up of gray fine sand with traces of cemented sand (loose to medium density). This layer's height varies too greatly and shows no consistency in the other borings.

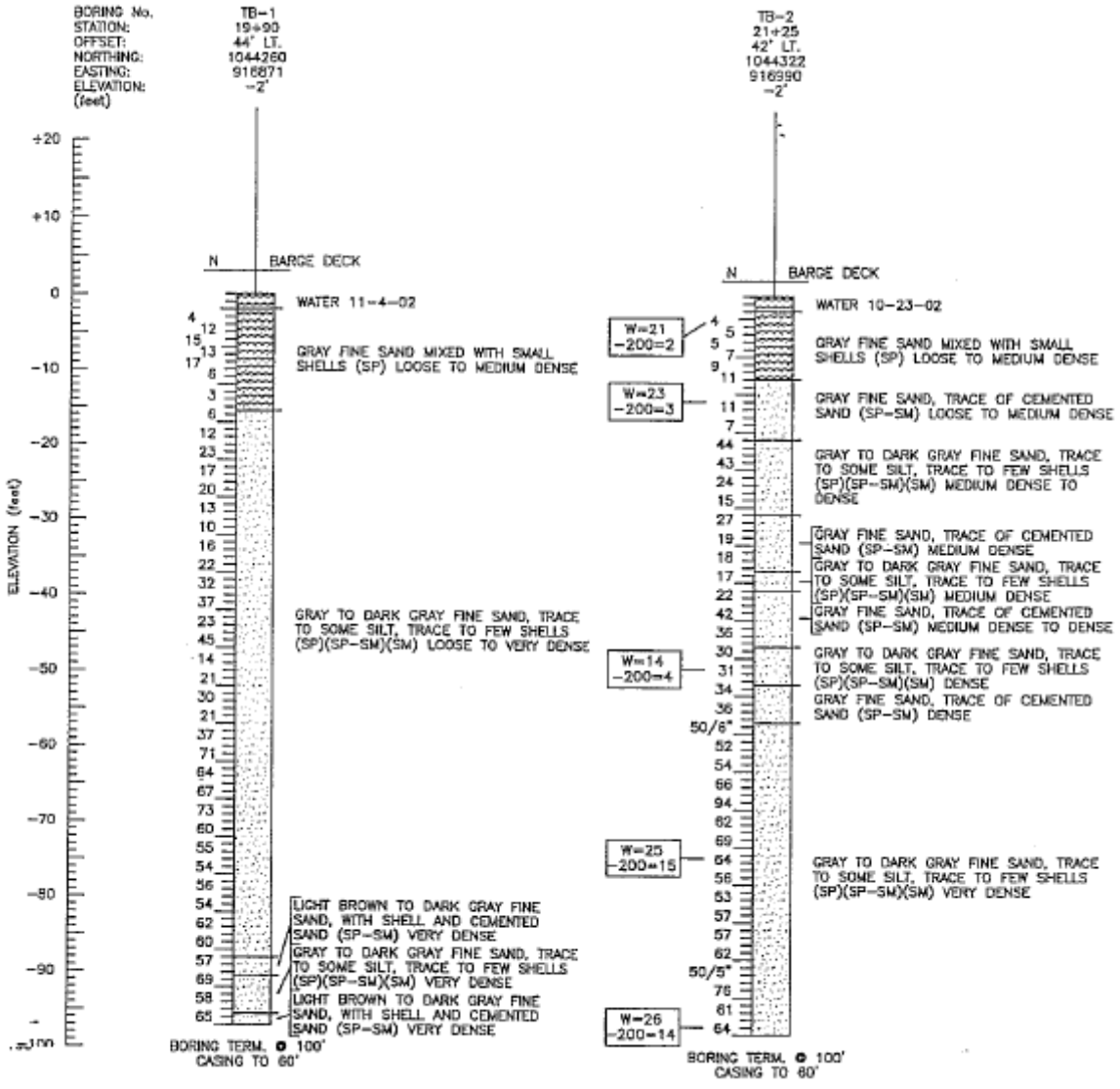

Figure 2.10 Borings "T-1" (left) and "T-2" (right) taken from bridge plans

The third layer shows the same type of gray to dark sand with evidence of silty material (loose to medium density). Starting from 55ft downwards, the soil becomes denser with a SPT "N" number greater than 50. In terms of density, the continue decrease in elevation shows an increase in density.

In the FB-Multipier software, there is a built in function for inputting the N numbers for the software to determine internal friction angle (phi) for cohesionless soils. For the purpose of, this function will be utilized. The soil springs associated with the soil data input are already incorporated into the model. There is also a function to override this by inputting user-defined soil spring constants. By doing so, the most accurately prediction of soil behavior can be obtained. An average internal friction angle of 36.2 degree is determined from inputting data from soil borings mentioned.

From inputting the internal friction angle into the software, built-in P-Y curves can be obtained. These are built-in lateral pile-soil interaction sand models that are needed to perform the P-Y Analysis. They are obtained through conducting large scale experiments. First, consider a pile not experiencing any force; the only forces are the normal uniform stresses from the soil acting along the length "x" of the pile. When a lateral load is applied, the pile will deflect and the soil stresses will not remain uniform but instead become larger due to applied loading. Figure 2.11 illustrates this simple procedure.

By doing this for different magnitudes of lateral load, different deflections are measured. Using these values, P-Y curves are established. These curves are nonlinear and are solely dependent on the soil type, embedment depth, pile cross-section, and pile surface roughness. The P-Y curves are specific for different piles in different soils with variations due to pile geometry, surface roughness, embedment length, tip type, and other factors. They are developed by researchers who conduct full scale experiments. They are essential in designing piles for bents and deep foundations. There are also dynamic P-Y curves which are determined by applying a dynamic lateral load rather than a static one. It is a rather more difficult process and it yields more realistic results. The act of a vessel impacting a bridge substructure is more dynamic in nature. A thesis conducted by (Bui 2005) shows the different between static and dynamic response of bridge piers due to vessel collision. To do so, dynamic P-Y curves were used.

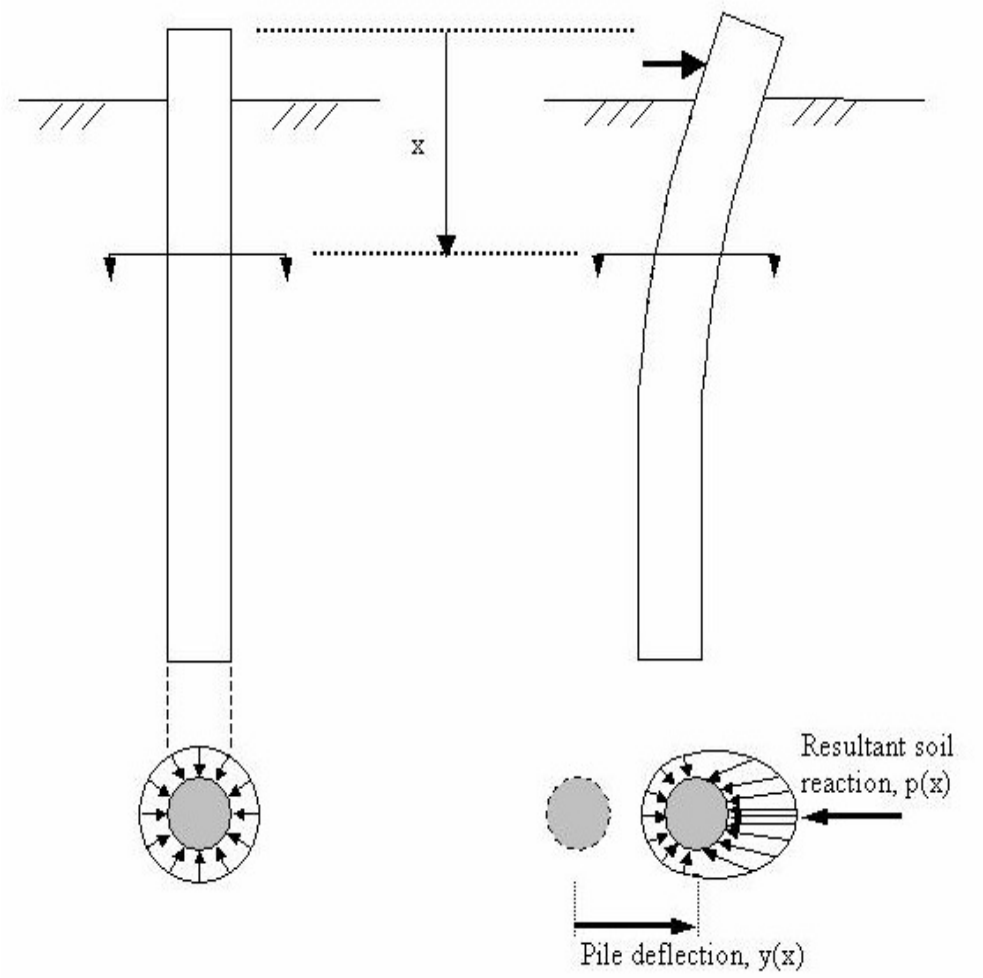

Figure 2.11 Demonstration of pile-soil interaction (FDOT)

The p-y curves used in this research are developed by (Reese et al. 1974). Figure 2.12 shows the p-y curves for the piles. The "N-#" signifies the node in the FB-Multipier model. Starting from node N67 (top of the pile) to node N57 and beyond (tip of pile), the lateral resistance becomes less and less. That indicates the deflection that will occur when a force is applied at that particular location. There can be infinitesimal curves for a single pile because there are infinitesimal points on the pile. For this particular finite model, each pile has roughly 20 nodes and thus there are 20 different curves in the plot witch each curve representing a different node (location) on the pile.

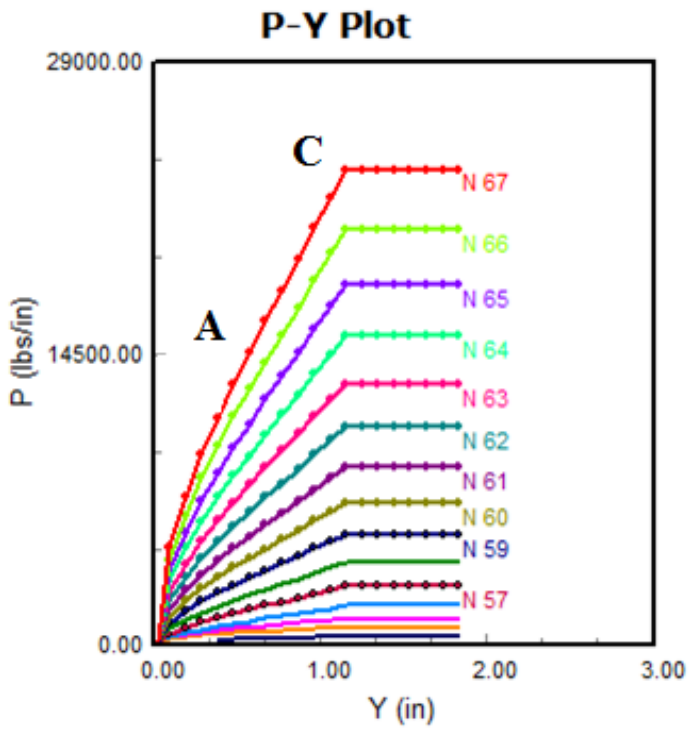

Figure 2.12 (Reese, et al) sand p-y curve

There are three portions to a P-Y curve. For this particular pile-soil interaction, the resultant P-Y curve does not resemble an ideal sand curve. Ideally, the first portion should be linear slope from the origin (0,0) to point "A". The second portion should be nonlinear from point "A" to point "C" and this is called the transition zone where the pile stops behaving elastically, instead behaves like plastic. The last portion from point "C" onward is the ultimate soil resistance (P_{ult}) of the pile where point "C" is the yield point.

To show the effect of scour on the lateral resistance of the pile, the unsupported length of the pile is increased (showing the effect of scour) and the resistance is recorded. The following Figure 2.13 shows the top node (N57) lateral resistance as scour depth increases. This node is the tip of the piles and it is picked because it shows the largest deflection in the entire pile.

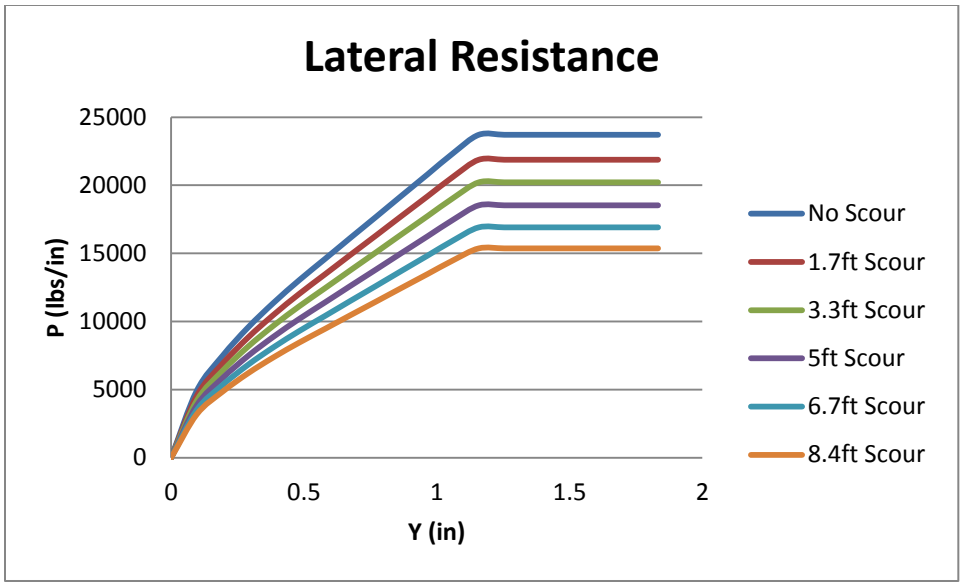

Figure 2.13 Lateral Pile Resistance for various scour depths

From an obtained coefficient of determination so close to one (0.9958), it can be concluded that the lateral resistance decreases linearly with the increase of scour. The rate at which the lateral resistance decreases versus scour depth seems to be a decreasing linear function. The rate at resistance decrease is 0.3% per inch of scour depth.

Laterally loaded piles are analyzed using the Euler classic beam theory to represent pile behavior and "p-y curves" show the nonlinearity of load transfer between the pile and soil (Anderson et al. 2003). The method basically replaces the soil with nonlinear springs and the pile is divided into equal smaller lengths. The following shows the classic beam theory used to analyze laterally loaded piles:

$$\frac{d}{dx^2}\left(E_p I_p \frac{d^2y}{dx^2}\right) + P_x\left(\frac{d^2y}{dx^2}\right) - p(x,y) - W(x) = 0$$

Where p_x = axial load on pile

y = lateral deflection of the pile at certain location of the pile's length

p(x,y) = soil resistance per unit length

W(x) = distributed load (hydrodynamic force, impact force, etc.)

E_pI_p = flexural stiffness

This is solved based on the finite difference method. In this case, the axial load is equal to zero. The lateral resistance of the piles and piers are based on unit length versus deflection. The lateral resistance is dictated by the p-y curves defined in previous section. In general, the pile is discretized into smaller lengths and the soil around them is discretized into springs. The spring is responsible to provide local resistance to the pile. In common practice, the ultimate lateral capacity of the piles is not important but the maximum deflection of the pile due to service loads (Poulos and Davis 1980).

Researchers used many approaches to analyze laterally loaded piles. Scoured piles are also analyzed the same way as laterally load piles except for the increase length (Bennett 2012). Scoured piles show definitely decrease in lateral resistance. These approaches have become simplified where they considered certain parameters such as boundary conditions. One simplified approach deals with analyzing piles with either pinned or fixed connections. As previously mentioned, the vessel impact force is to be applied as a static force parallel to the substructure (longitudinal direction), there are some discrepancies as to whether the pile's head is pinned or fixed. Another load location dictated by the guide is 50% of impact force striking substructure in the transverse direction, it is justifiable to say that the pile's head is definitely fixed because the bridge span/decking provides the fixity. In both scenarios, the pile is likely considered fixed to the pile cap. According to researchers, it is better to design piles to have fixed connections because fixed head piles are able to provide twice the lateral resistance compared to free headed piles (Paduana and Yee 1974). Fixed headed piles also perform better in terms of deflection; they are able to deflect one fourth that of free head piles (Kim 1984). Also, they are able to transfer bending between the superstructure and substructure. In FB-Multipier, only fixed head situations will be assessed.

2.6 Fixity Depth

The fixity depth is the depth below the top of the soil that exhibits a fixed connection behavior. It is the depth at which the soil provides enough resistance that fixes the pile to the soil. This is considering the pile to be partially embedded which equals to a free-standing pile with a fixed base. When scour occurs, the unsupported length of the pile is increased. The pile is

modeled as a cantilever and pile bents as frames. The following equation shows numerically how the depth of fixity (point of fixity) is determined below the ground level of a partially embedded pile in sand:

$$L_f = 1.8\sqrt[5]{\frac{EI}{n_h}}$$

Where L_f = depth of fixity below the soil top

E = modulus of elasticity of the pile

I = weak axis of moment of inertia

n = rate of increase of subgrade modulus for sand

Using this point of fixity approach, the soil is assumed to be elastic (Robinson et al. 2011). According to this author, researchers and engineers consider the point of maximum negative moment as the point of fixity. The 1.8 in the equation exists to account for the bending and buckling response simultaneously. The negative drawback is the singularity of this method; for multiple layers that contain different soil types, an equivalent soil layer must be determined to use this equation. Fortunately, the soil profile around the West Island Access Bridge is made up sand layers. The following table (Table 2.1) taken from (Chen 1997) shows the accepted n values for sands:

Table 2.1 n_h values for differrent sand types

Sand Type	Saturation Condition	n
Loose	Moist/Dry	30
	Submerged	15
Medium	Moist/Dry	80
	Submerged	40
Dense	Moist/Dry	200
	Submerged	100

The same author (Bennett 2010) in another paper states that the soil properties can change when scour occurs so the stress history of the soil needs to be considered. This means the soil can change from being normally consolidated to over-consolidated. For simplicity of this research, this will not be investigated but rather mentioned for its importance.

Using the information mentioned above, a point of fixity value of approximately 6.3ft is determined. That is the average of the two values obtained using the n_h values of 40 and 100 of the submerged saturation condition of the medium and dense sand types respectively. The fixity depth will be used as a point of observation; to observe the changes in moment and shear. Before this can be done, it needs verification because the piles in the model are fixed to the pile cap as opposed to free condition this fixity approach states. One way to verify this is to determine the fixity depth by located the change in maximum negative moment. If the values are similar then this fixity approach also works for fixed head condition. Table 2.2 shows the fixity depths for each scour level. The first column shows the scour depth which starts from zero and increases with a portion of the equilibrium scour and proceeds beyond that value. The second column shows the elevation of the soil top when the said scour has occurred. The last column shows the location of the calculated fixity depth based on the elevation of the soil top.

Table 2.2 Calculated depth of fixity for each scour level

Scour Depth (ft)	Soil Layer Top Depth (ft)	Fixity Depth (ft)
0.0	16.0	22.3
1.7	17.7	24.0
3.3	19.3	25.6
5.0	21.0	27.3
6.7	22.7	29.0
8.4	24.4	30.7
11.0	27.0	33.3
14.0	30.0	36.3
15.0	31.0	37.3
20.0	36.0	42.3
23.0	39.0	45.3
27.0	43.0	49.3

2.7 FB-MultiPier

FB-MultiPier is a nonlinear finite element analysis program designed especially for analyzing bridge pier structures either as full bridge spans, single piers or pile bents. The software is capable of performing nonlinear finite element analyses on substructures with nonlinear soils for axial, lateral, and torsional soil behavior. In general, a linear system differs from a nonlinear system by the output these systems produce. A linear system's output is directly proportional to its input while a nonlinear system's output it not proportional to its input and will not satisfy the principle of superposition. For linear behavior, the software assumes pile behavior is purely linear elastic; this is never the case especially when it comes to high magnitude forces. For nonlinear approach, P-delta moment (moments resulting from axial forces) is considered in the analysis. This software is well suitable and capable of analyzing structures like bridge piers and entire bridge due to the nonlinear behavior of piles. According to (Robinson et al. 2011), FB-Multipier can properly determine response of nonlinear piles such as point of fixity. This was proven in their findings based on three case studies.

The elements available in the software include beam elements used to model piles, girders, and plate elements used to model shearwalls between large pier columns, pile caps, and decks. For this particular model, only beam elements are used. The piles are divided into 20 equally long elements with each approximately 2.79ft long. Figure 2.14 shows an orthogonal view of the model. The length of the elements changes as the scour depth changes. 15 nodes are in embedded within the soil profile while 5 nodes are free. In the manual, it states that 17 pile nodes are sufficient enough to model soil response and give accurate results. When a new scour depth has occurred, the nodes readjust with different element lengths. The top 5 elements will increase in length due to the increased unsupported length and 15 elements in the soil will decrease in length due to the decrease soil depth due to scour. The sixth node from the top is the location of the soil top. Also, the pile cap is able to move freely. One way to hinder this movement is to add springs to the pile cap nodes.

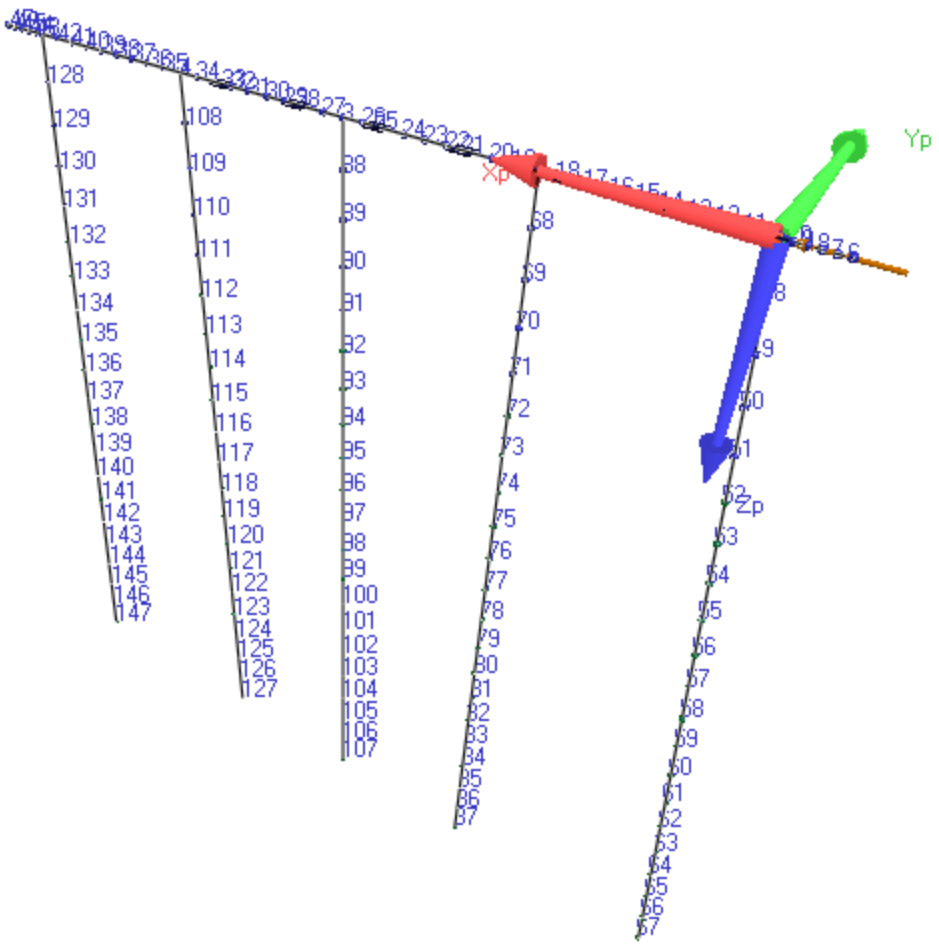

Figure 2.14 FB-Multipier pile bent finite element model

The pile cap consists of 40 nodes. Eight nodes exist between the piles with 4 nodes in the cantilever section. Having more elements/nodes will yield more accurate results but the run times will take significantly longer to compute. The number of element in the model is sufficient enough to give accurate readings at reasonable computation times. The output results indicate the beginning and ending depths of an element and the associated demand/capacity, shear, and moment values. For each increment of scour depth, the model is re-assessed and regenerates the elements with equal lengths, retaining the same node notations.

The global coordinate system comprises of the red arrow representing the x-axis, green arrow representing the y-axis, and the blue arrow representing the z-axis (increasing downward). For the piles, the 2-axis corresponds to the global x-axis while the 2-axis corresponds to the global negative y-axis. When the lateral load is applied, only 2-axis (x-axis) will experience moment so for keeping things simple, the axis specific moment notation will be ignored, instead only the moment that occurs will be discussed. Thus, the moment and shear results of the piles reported are for the global coordinate system of the model. There is no function in the software to assign a local axis different from the global. The program automatically assigns the global axis.

2.8 Demand/Capacity

Demand/capacity ratio is a value between zero and one that shows how much capacity is used to resist the demand. The demand is the force distributed to the piles which is determined by finite element analysis conducted by the software. Capacity is how much strength the piles provide and is calculated using the following combined axial and bending interaction equation:

$$\frac{P_u}{\Phi P_n} + \frac{M_u}{\Phi M_n} \leq 1.0$$

Where P_u = factored axial compression load

M_u = factored bending moment

P_n = nominal axial strength

M_n = nominal bending strength

The demand/capacity ratio of the system is how much capacity the substructure provides in terms of the required moment and axial demand. The FB-Multipier software automatically computes the moment demand & capacity of the pile bent based on the reinforcement of the piles and pile cap. Some results will show ratio values over 1.0. The reasons behind this are simple; the program doesn't take into account the tensile strength of concrete when the capacity is computing but instead takes into account the minimal tension in concrete during the computation of the demand (Institute 2000).

Also, hinges are formed at quarter points at both ends of the element which actually has demand/capacity ratios of 1.0 but the element forces developed at these quarter points which are then extrapolated to give values at the element's ends. That creates the possibility for values greater than 1.0 to be developed at the ends. Both of these reasons contribute to a more conservative method.

2.9 Increased Battered Ratio

In general, piles are just columns supporting a structure. Like columns, they exhibit column behavior which provides resistance in terms of moment and axial force. Previously mentioned, pile bents are evaluated as rigid frames. Having battered piles allow the piles to resist the lateral using some of its axial resistance. This is dictated by the interaction diagram. Non-battered piles exhibit pure moment resistance. During the scour process, moment demand is increased due to the increase in moment arm. If the moment arm is the distance between the lines of action of the force to the fulcrum point then battered piles will experience shorter moment arms due to their geometry. The benefits of having battered piles benefit in the terms of moment demand and also the increase in axial resistance.

2.10 Scenarios

Three scenarios will be assessed. The first one is during the normal flood conditions which include scour and hydrodynamic force. The second scenario is during the extreme load event which includes scour, hydrodynamic force, and vessel impact force. Due to the small magnitude of hydrodynamic force compared to the impact force; the hydrodynamic force will be neglected. The last scenario is similar to the second one except the battered ratio will increase to 1:4. This is to address the correct ratio for pile bents designed for minor vessel impact. In this case, the vessel impact isn't minor but the code does not state a value for major vessel impact. Bridges prone to major vessel impact have large pier substructures rather than pile bents. Needless to say, major vessel impact can happen to small bridges with pile bent substructures. Initially, the model will run under scour inducing normal flood conditions. The results will be recorded and used as the control. The sequential runs involve applying the vessel impact force during the extreme load event for the two different battered ratios.

CHAPTER THREE

RESULTS AND DISCUSSION

3.1 Fixity Depth

The software chooses the node closest to the actual depth to the fixity depth. As previously mentioned, one way to determine the fixity depth is the location of change in maximum moment in the pile. From looking at the moment results, these depths are determined. This is shown highlighted in the each of the tables identifying this change in the appendix. One fact discovered is that the fixity depth is the same for all the piles in the bent. That means they all show signs of change in maximum negative moment. There are data showing other different depths in other piles that show change in maximum negative moment but not at the same depth for the other piles. These elevations are not the fixity depth. That is assuming equal scour occurs at all the piles. This becomes more evident during the extreme loading. Table 3.1.1 compares depth values from all three situations to the values previously calculated using the empirical equation.

From the looking at the numbers, the depths during the normal flood and extreme event are identical with the exception of the first value. This does not necessary mean that the depths are not the same when there is no scour because the software does not take into account which run is considered scoured or unscoured; it's considered relative what is set by the user. By changing the battered ratio, the locations of fixity change. This perhaps hints at the idea that the fixity depth depends on the orientation of the piles or it may be that the different battered ratio affects the element lengths in the soil and the software chooses the node closes to the depth which happens that the node location is different from the one in the previous battered orientation. All the values are different from the other two situations. The calculated and determined values are not exactly the same but are close enough. The difference may be caused by the number of nodes. By increasing the number of nodes, the software is able to pick a node even closer to the actual fixity depth. Nonetheless, the fixity depths are used to monitor the changes.

Table 3.1 Comparison of calculated and determined depths

Calculated Depth (ft)	Normal Flood (ft)	Extreme Event (ft)	Extreme Event (ft) Increased Battered
22.3	21.441	24.161	23.866
24.0	25.521	25.521	25.226
25.6	26.801	26.801	26.506
27.3	28.161	28.161	27.866
29.0	29.521	29.521	29.226
30.7	30.881	30.881	30.586
33.3	32.961	32.961	34.554
36.6	-	37.148	36.754
37.3	36.161	-	37.487
38.3	-	-	38.221
39.3	-	-	38.954
42.3	40.161	-	42.443
45.3	-	-	44.443
49.3	-	-	47.931

3.2 Deflected Shape

The shear and moment of each pile are distinguishable and show signs of symmetry due to the dominant distributed dead weight of the pile bent but somewhat exhibit skewness due to the hydrodynamic force striking pile#1 which is shown in Figure 3.1. This becomes more evident when comparing deflection shape of the two scenarios. Figure 3.3 shows that symmetry doesn't exist in the extreme event due to the high magnitude of vessel impact striking the side of the pile bent. For the extreme load events, the model was analyzed for scour depths up until the pile bent became unstable and the results could not be viewed. Against 50% of the design vessel load, the pile bent can withstand up to 14ft of scour. By increasing the battered ratio from 1:12 to 1:4 (horizontal to vertical), 27ft of scour can occur until the pile bent becomes unstable. The following diagrams show the deflected shapes of the pile bent under the two scenarios at 5ft of scour. Under the normal flood conditions, the pile bent deflects in compression due to the weight of the pile cap being larger than the hydrodynamic force. Under the extreme load event, the bent experiences sidesway which is expected for rigid frames with lateral loading.

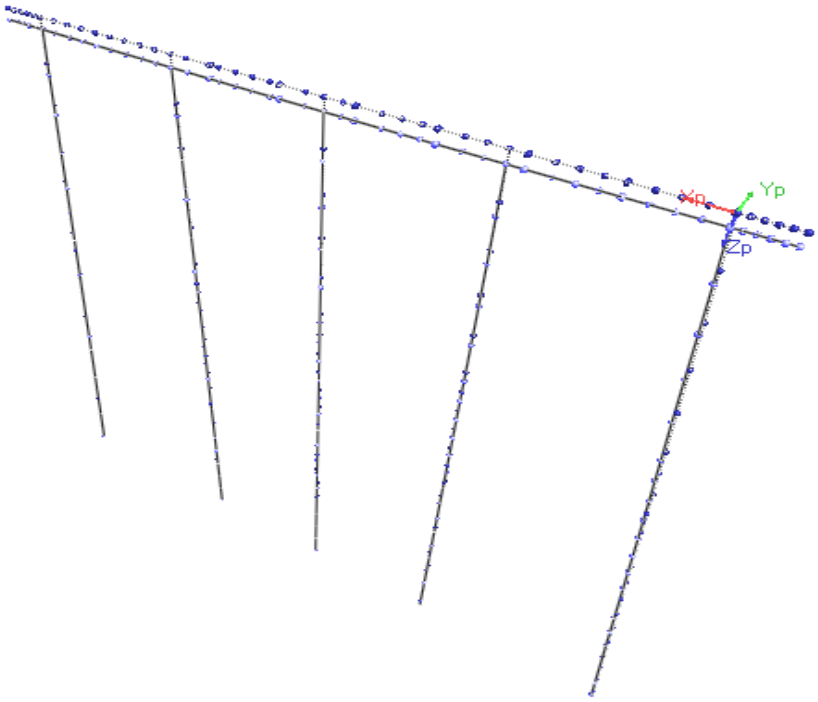

Figure 3.1 Deflected bent shape during normal flooding

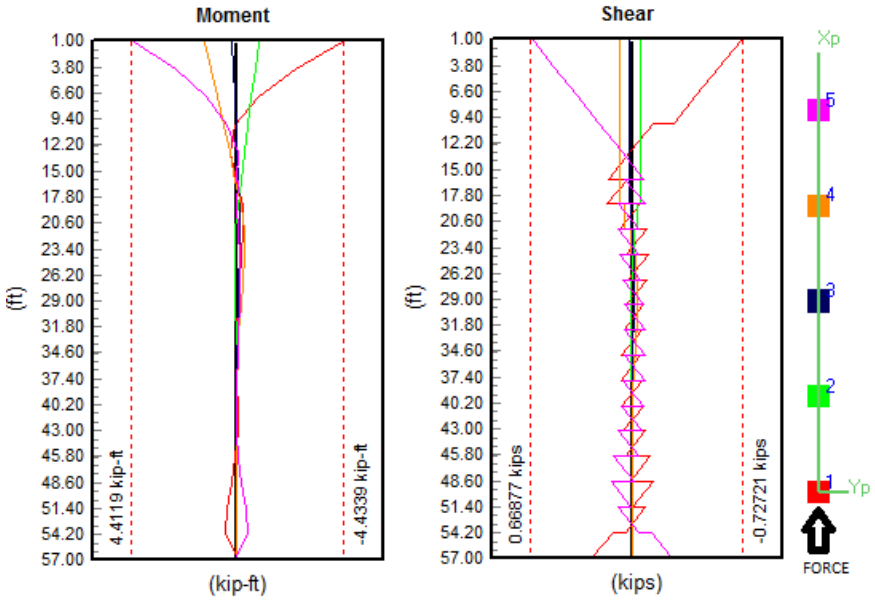

Figure 3.2 Moment and shear diagram with plan view of piles during normal flooding

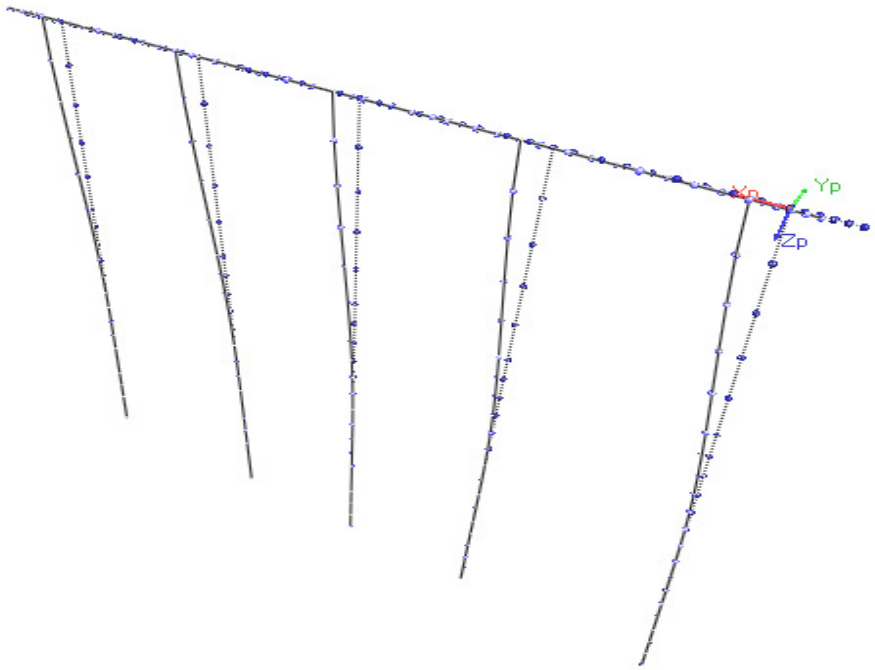

Figure 3.3 Deflected bent shape during extreme loading

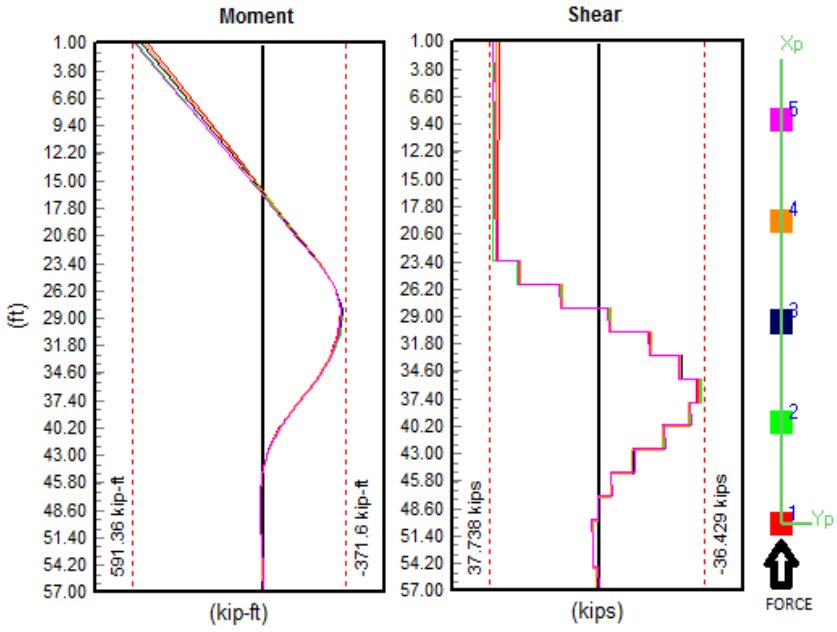

Figure 3.4 Moment and shear diagram with plan view of piles during extreme loading

3.3 Moment

The piles all show the same magnitude of moment at the fixity location during early stages of scour but begin to diverge as scour becomes more severe. The first pile where the impact force struck doesn't necessarily show that it induces the most moment but the most moment lies in the fifth pile, away from the force. Figure 3.5 shows that during normal flooding, the middle piles receive the least moment while pile#1 receives the highest negative moment and pile#5 receives the highest moment in the opposite direction. This is due to the deadweight of the pile bent. The lower moment values in the middles are a direct result of the hydrodynamic force; no moment is caused from the deadweight of the bent, while the first and last pile are a result of the hydrodynamic force and the p-delta effect from the bent's deadweight due to the battered nature of the end piles.

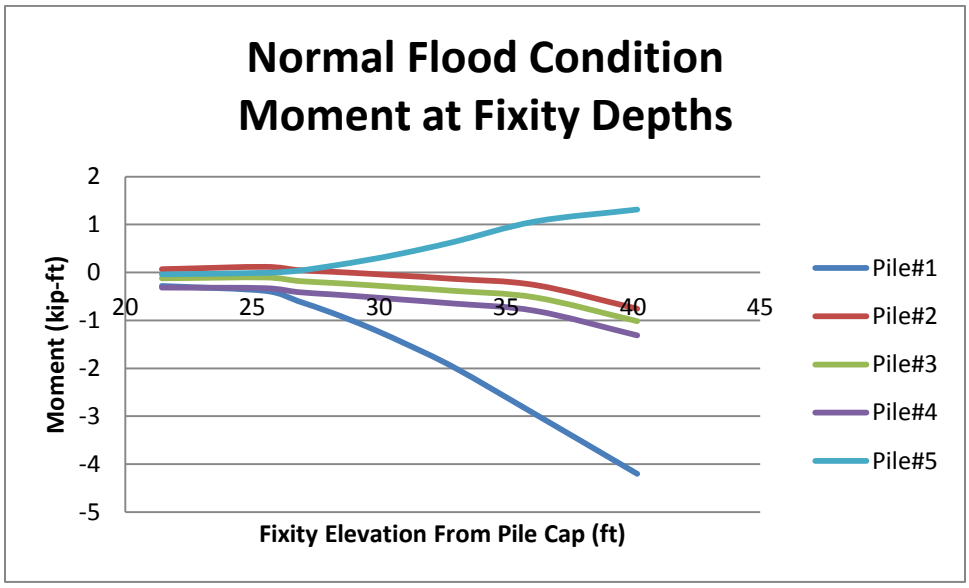

Figure 3.5 Moment at different fixity depths (normal flood scenario)

For extreme event (battered ratio 1:12), Figure 3.6 shows the moment at different fixity depths. The moment is distributed equally during the early stages of scour and begins to diverge during the later severe stages. The fifth pile receives the most moment.

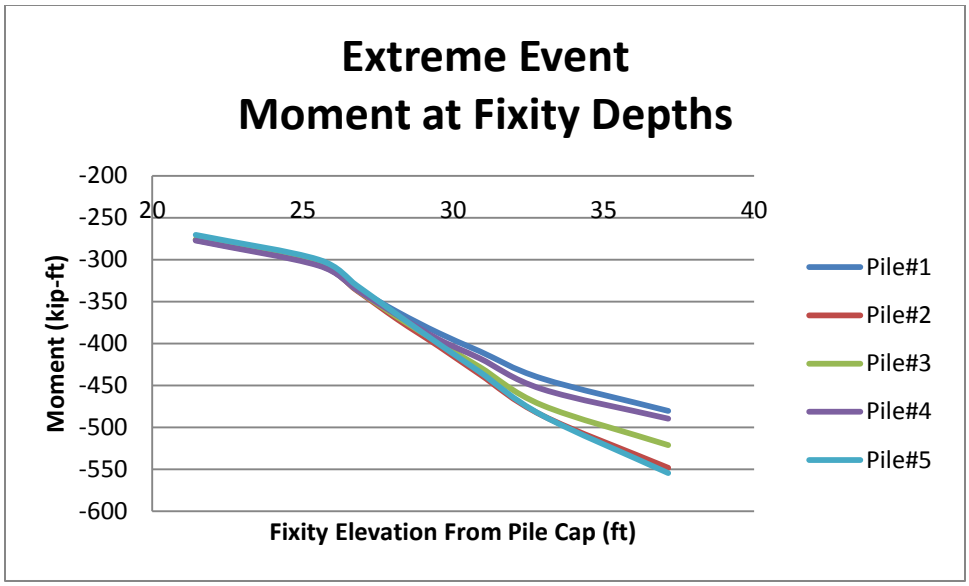

Figure 3.6 Moment at different fixity depths (extreme load event scenario)

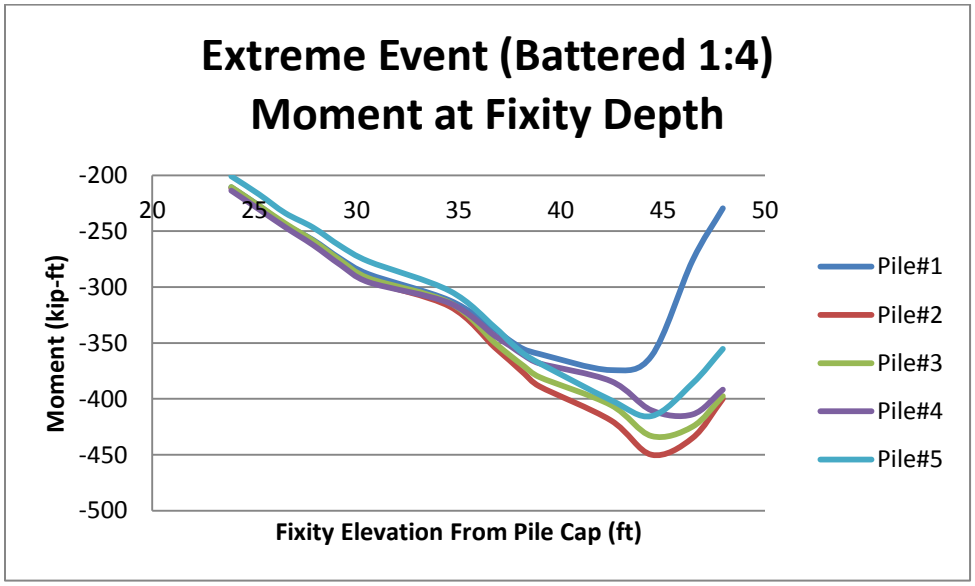

Figure 3.7 Moment at fixity depths (extreme load event-increased battered ratio)

The increased battered ratio allows the pile bent to handle more scour and provide more capacity but approximately 2-3ft before the bent topples over, the bent experience a decrease in moment. There isn't enough embedded depth for the bent to develop any fixity. That explains the

sudden decrease in moment near those locations. The following demand/capacity also shows a decrease in demand at those depths. Since the capacity of the piles cannot be directly calculated because demand/capacity is based on interaction of the axial and bending stresses.

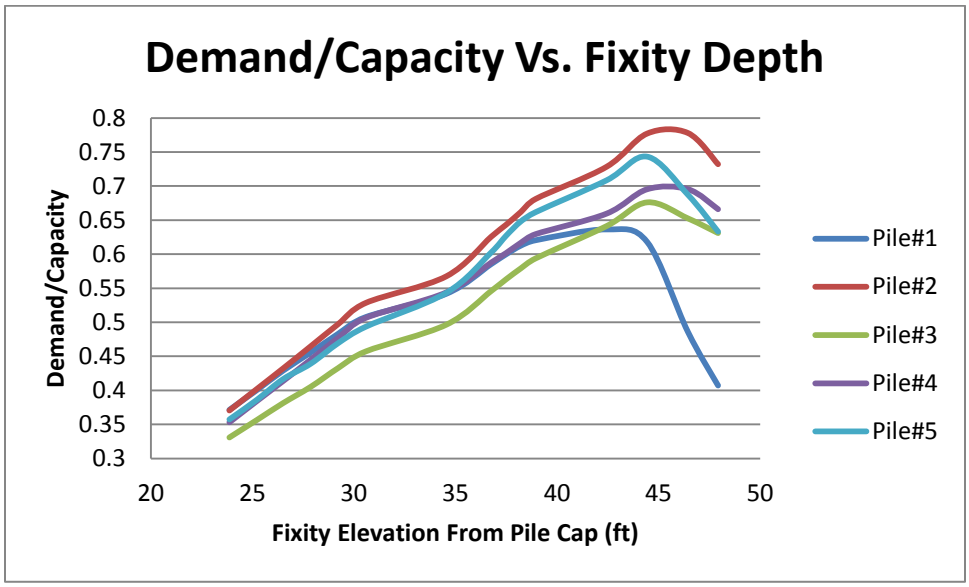

Figure 3.8 Demand/Capacity vs. Fixity Depth (extreme event-increased battered ratio)

At the location of the top of the piles, the moment increases substantially where the fixity depth reaches that elevation between -45ft to -50ft. The sudden decrease in moment at the fixity depth becomes a sudden increase in moment at the pile cap. One educated explanation would be that at those depths, fixity decreases due to the inadequate embedded length of the pile. The more fixed (stiff) portion of the pile bent exists at the pile cap. Stiffer members tend to attract load. Another explanation would be the pile has reached its yield point and no longer exhibits elastic behavior and begins to act plastically. Therefore the piles no longer follow the classic beam theory. To soundly arrive at a conclusive explanation, more research needs to be done. The entire bridge or portion of the bridge needs to be modeled. This is one recommendation for future research. At this point, it is rather difficult to arrive at a solid conclusion.

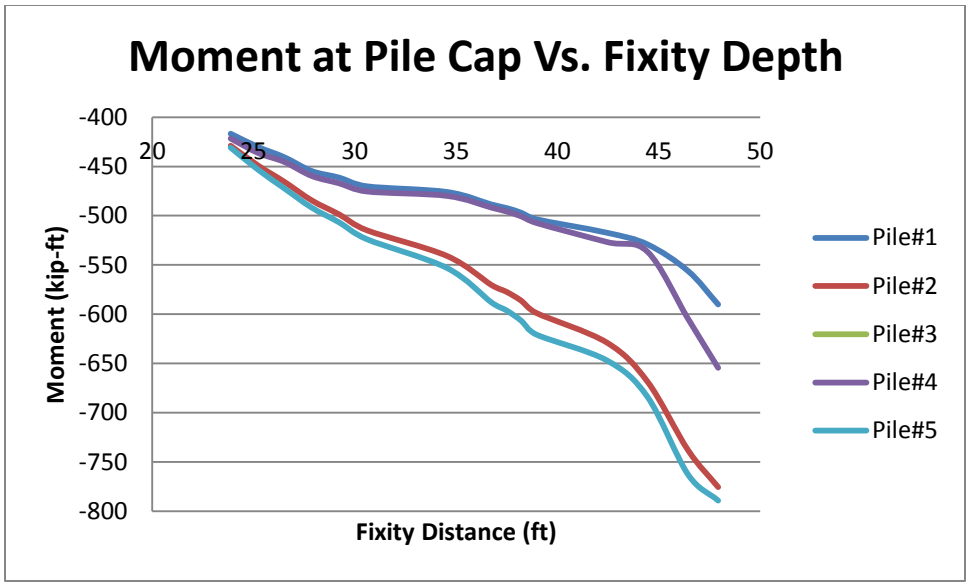

Figure 3.9 Moment at pile cap (extreme event-increased battered)

The tip of the piles experiences practically zero moment. The end battered piles in all situations experience very little moment. In the normal flood conditions, the end battered pile tips show the same magnitude of moment. This is due to the dead weight of the structure. During the extreme load event, that behavior changes and there is not any consistency as the values appear random. Maximum positive and negative moment exists at the pile cap in both normal flooding and extreme loading. Maximum positive moment exists at the pile cap while negative maximum exists at the fixity depth.

3.4 Shear

Upon initial observation of shear forces between the two situations in Figure 3.10, the maximum occurs at the soil layer top and not at the fixity depth during the extreme event. The shear of the end piles during the normal flood condition shows unusual behavior, one that doesn't follow Euler's classic beam theory. It shows the shear maximum occurring at the pile top which is partially true. The shear should start from top of the soil and remain constant up to the pile cap but instead it increases along the length of the pile to the top. For 5ft of scour, the resultant hydrodynamic force is applied at approximately 12.3ft. At this point, there is a sudden increase in shear which makes sense because shear increase just to the left and right of the

applied load. From there, it continues to increase along the length of the pile to the pile cap. Perhaps this is due to the 3ft overhang of the pile cap and since the pile cap deadweight is larger than the hydrodynamic force, it creates unusual load transfer. Also, if the shear diagram for the end battered piles is tilted, it shows a shear diagram expected for a beam loaded approximately in the middle. This leads to the question whether the software FB-Multipier assumes a local axis for the end batter piles. In the previous section 2.7, it is stated that the software analyze the model according to its global axis. This occurrence in shear behavior of the end piles during the normal condition needs further research to arrive at a more solid conclusion.

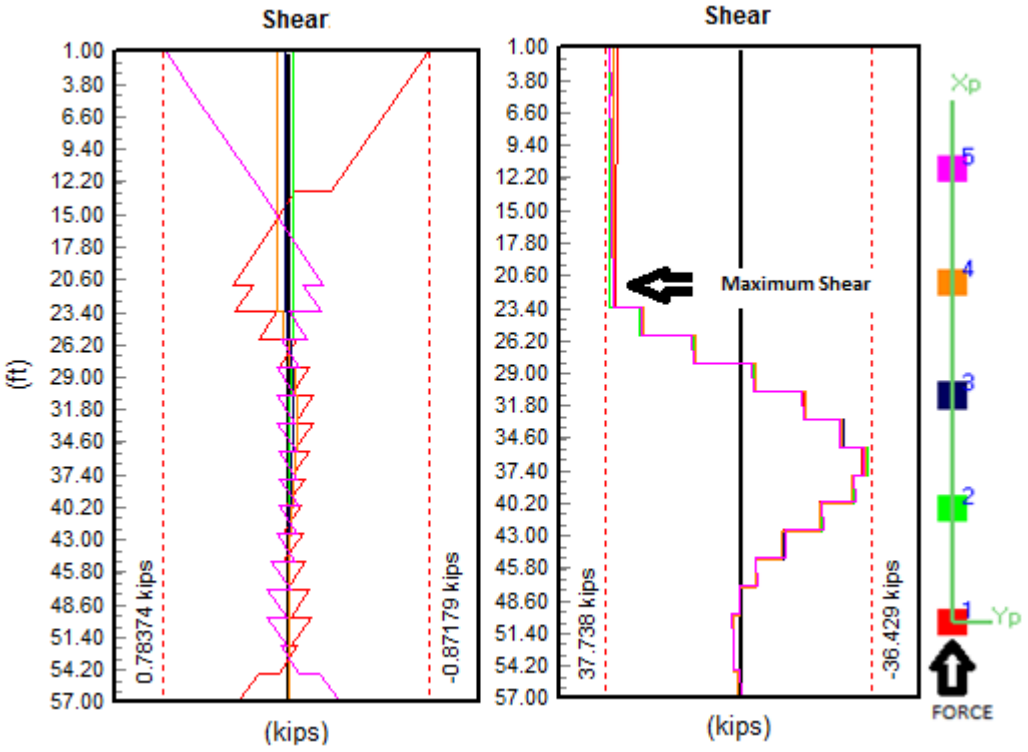

Figure 3.10 Comparison of shear between normal flooding and extreme loading (5ft)

Focusing more on the extreme load events, the maximum shear occurs at the top of the soil and the fixity depth is where the shear force goes from negative to positive or vice versa. Similar to moment, majority of the shear occurs at the pile cap. Unlike moment distribution

which the piles show some consistency, shear distribution seems to be completely random. Figure 3.11 shows the randomness of shear distribution to the piles at the top of soil. Vessel impact definitely increases the shear at the base and pile top. The sum of the shear of all the piles roughly equals to the applied lateral force of 200 kips (battered ratio 1:12) which is expected since the all the piles are vertical with the exception of the end piles but that battered ratio is rather small.

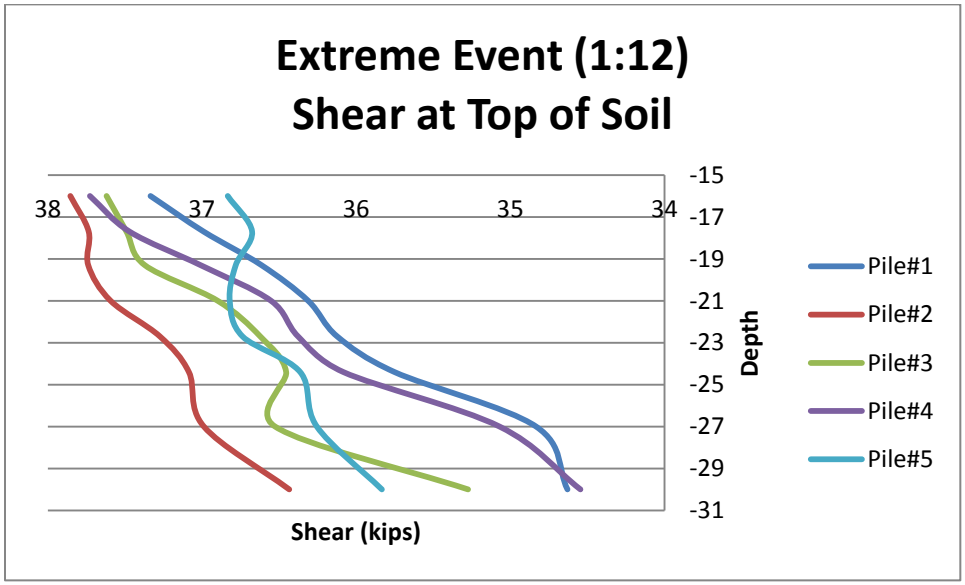

Figure 3.11 Shear at top of soil layer-extreme loading

By increasing the battered ratio to 1:4, the randomness lessens. The overall maximum shear decreases and the piles show approximately the same magnitude and not much variance. The sum of the shear of all the piles roughly equals less than the applied lateral load. This is due to the increased battered ratio of the end piles; some of shear has transformed to moment due to the increase eccentricity. The ratio 1:12 is perhaps too small to allow any substantial change. Piles 1 to 4 show some signs of consistency with values ranging from 28 to 31 kip. As the scour becomes severe, the shear in the piles diverges. The fifth pile however, receives the least amount of shear and starts to decrease substantially as scour becomes severe. This correlates with the sudden decrease in moment. The reasons for occurrence may be also similar.

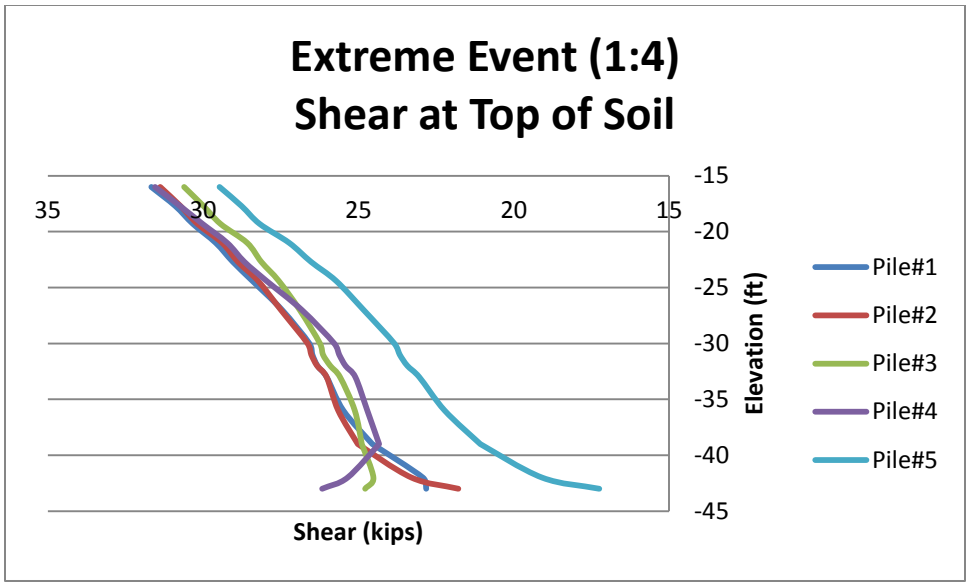

Figure 3.12 Shear at top of soil layer-extreme event increased battered

3.5 Demand/Capacity

During normal flood conditions, the maximum demand/capacity ratio occurs in middle pile which means that the dead weight of the substructure is larger than the hydrodynamic force. The reason lies in the pile interaction diagram. The middle pile experiences more dead weight and less moment caused by the lateral due to its location in the bent. The difference in their demand/capacity ratios isn't substantial but it gives a clear indication of this phenomenon. Comparing only the maximum demand/capacity ratio in the entire pile bent is enough to draw conclusions because the whole system is only as its weakest link. The maximum value occurs at the same node throughout the different scour depths. The demand of the system (the lateral force and dead weight) remains the same while the capacity of the system decreases during the occurrence of scour thus the ratio of demand/capacity increases. This is true for all situations. The following graph (Figure 3.13) shows the maximum demand/capacity values for each situation at different scour depths.

The curves show linear behavior between zero and one. Previously mentioned, the D/C value can be over 1.0 due to the software's habit to extrapolate to get values for the beginning and end of elements. Having shorter elements will help zone in on a more accurate answer. One

reason why the substructure does not fail immediately once it has utilized all its capacity is due help from the other parts (elements) of the substructure picking up the extra load demand. Eventually when enough elements have exceeded their capacity, the substructure will fail.

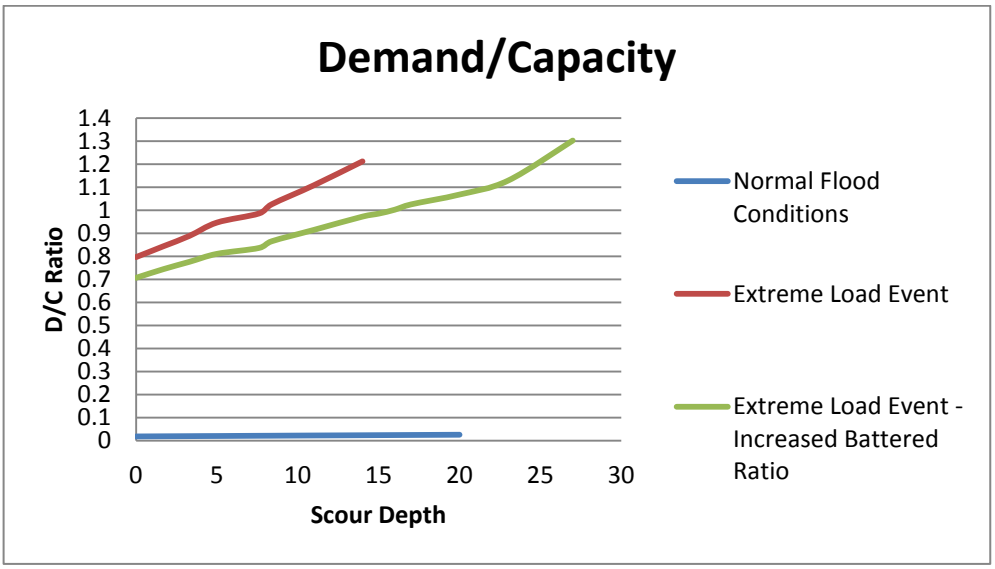

Figure 3.13 Pile bent demand/capacity at different scour depths

Having a 1:4 horizontal to vertical battered ratio definitely help increase the capacity of the system; it allows a better balance of combined axial and bending resistance of the piles. From the graph, the pile bent is able to maintain a constant 10% more capacity than a 1:12 battered ratio.

CHAPTER FOUR

CONCLUSIONS

4.1 Conclusion

The premise of this project was to investigate the static structural implications of a bridge substructure during an occurrence of an extreme load event. This such event is plausible when severe scour occurs during a 100-year storm and a drifting minimum design vessel defined as an empty hopper with dimensions 195ft x 35ft, tied to its moorings, suddenly breaks loose, and strikes the substructure. A particular substructure (pile bent) like in the Ernest Lyons West Island Access Bridge, Florida was chosen for this investigation because it had the readily available data needed. Utilization of the FB-Multipier software was the choice of analysis in this project due to its main function as a bridge structure/substructure analysis program capable of computing nonlinear finite element analysis. The overall methodology conformed to the AASHTO's LRFD Bridge Specifications and Vessel Collision Specifications Guide pertaining vessel impact and all necessary tools needed.

From the results and comparisons obtained in this work, a list of the following can be inferred:

1. During the scouring process, low magnitude hydrodynamic force alone is not enough to cause bridge failure especially in shallow mean water depth like the one in this project.
2. The location of the impact force on the substructure greatly influences the static changes.
3. During impact, maximum negative moment indeed occurs at the depth of fixity and maximum positive occurs at the pile cap where the pile is embedded in.
4. Shear on the other hand, occurs at the scoured depth and remains constant, decreasing slightly as it travels up to the pile cap.
5. Moment distribution shows signs of consistency in but shear distribution is rather completely random.

6. Increasing battered ratio of the end piles can improve performance of the pile bent by decreasing the demand/capacity ratio by 10%.

4.2 Future Research

One aspect that was not covered was pushover analysis. Pushover analysis is a simple method also known as nonlinear static analysis that can be applied to any structure that shows signs of inelastic behavior. This analysis method has an advantage over dynamic analysis methods such as Response History/Spectra because they do not account for nonlinear behavior of the deformations caused during the initial lower loads. Basically, this method is used to obtain the ultimate load carrying capacity of the pile bent under severe loading such as high hydrodynamic forces and impact forces. The piles are first discretized into smaller elements connected through nodes. A minimum load is selected and applied to the pile. The deformations at the location of the nodes are noted. Among these nodes, one is selected as the control node. In this case, the top of the pile bent is selected as the control node because of that node's tendency to deflect the most in the entire structure. The structure experiences deformation during low magnitude of applied loading and will continue to experience deflection from increased loading magnitude in a nonlinear manner. The method is complete when the ultimate deformation is exceeded. All the results are plotted as a curve called the "pushover" curve. In the FB-Multipier software, there is a built-in function that completes a pushover analysis just by inputting number of steps and load increment factor. This can be done for future study.

Another thing to consider is modeling an entire bridge or portion of bridge (superstructure and substructure) to observe the changes that occur during the three scenarios. When the pile bent fails, the adjacent bents are required to resist more force. An entire bridge model can also provide insight on the superstructure's role in resisting the impact force.

APPENDIX A

SAMPLE NORMAL FLOOD CONDITION DATA

Shear values with no scour

Elevation (ft)	Pile 1 Shear (kips)	Pile 2 Shear (kips)	Pile 3 Shear (kips)	Pile 4 Shear (kips)	Pile 5 Shear (kips)
1	-0.7272	-0.0508	0.0183	0.0884	0.6688
4	0.5772	0.0508	-0.0183	-0.0884	-0.5188
4	-0.5772	-0.0508	0.0183	0.0884	0.5188
7	0.4272	0.0508	-0.0183	-0.0884	-0.3688
7	-0.4272	-0.0508	0.0183	0.0884	0.3688
10	0.2772	0.0508	-0.0183	-0.0884	-0.2188
10	-0.1377	-0.0508	0.0183	0.0884	0.2188
13	-0.0123	0.0508	-0.0183	-0.0884	-0.0688
13	0.0123	-0.0508	0.0183	0.0884	0.0688
16	-0.1623	0.0508	-0.0183	-0.0884	0.0812
16	0.0333	-0.0508	0.0183	0.0884	0.0477
18.72	-0.1693	0.0508	-0.0183	-0.0884	0.0884
18.72	-0.0516	-0.0344	0.0067	0.0484	0.0942
21.441	-0.0845	0.0344	-0.0067	-0.0484	0.0418
21.441	-0.0958	-0.0136	-0.0052	0.0033	0.0958
24.161	-0.0402	0.0136	0.0052	-0.0033	0.0402
24.161	-0.1065	0.0027	-0.0118	-0.0265	0.0788
26.882	-0.0295	-0.0027	0.0118	0.0265	0.0572
26.882	-0.0971	0.0108	-0.0126	-0.0362	0.0611
29.602	-0.0390	-0.0108	0.0126	0.0362	0.0749
29.602	-0.0811	0.0118	-0.0095	-0.0312	0.0507
32.323	-0.0549	-0.0118	0.0095	0.0312	0.0854
32.323	-0.0675	0.0088	-0.0054	-0.0198	0.0484
35.043	-0.0685	-0.0088	0.0054	0.0198	0.0876
35.043	-0.0606	0.0048	-0.0020	-0.0090	0.0521
37.764	-0.0754	-0.0048	0.0020	0.0090	0.0839
37.764	-0.0618	0.0017	0.0000	-0.0018	0.0603
40.484	-0.0742	-0.0017	0.0000	0.0018	0.0758
40.484	-0.0723	-0.0001	0.0007	0.0015	0.0739

43.204	-0.0637	0.0001	-0.0007	-0.0015	0.0621
43.204	-0.0935	-0.0007	0.0007	0.0021	0.0957
45.925	-0.0425	0.0007	-0.0007	-0.0021	0.0404
45.925	-0.1227	-0.0006	0.0004	0.0015	0.1242
48.645	-0.0133	0.0006	-0.0004	-0.0015	0.0118
48.645	-0.1406	-0.0003	0.0002	0.0007	0.1413
51.366	0.0046	0.0003	-0.0002	-0.0007	-0.0053
51.366	-0.0923	-0.0001	0.0000	0.0001	0.0924
54.086	-0.0438	0.0001	0.0000	-0.0001	0.0436
54.086	0.1274	0.0000	0.0000	-0.0001	-0.1276
56.807	-0.2634	0.0000	0.0000	0.0001	0.2636

Shear values during 5ft of scour

Elevation (ft)	Pile 1 Shear (kips)	Pile 2 Shear (kips)	Pile 3 Shear (kips)	Pile 4 Shear (kips)	Pile 5 Shear (kips)
1	-0.8718	-0.0269	0.0272	0.0829	0.7837
5	0.6718	0.0269	-0.0272	-0.0829	-0.5838
5	-0.6718	-0.0269	0.0272	0.0829	0.5838
9	0.4718	0.0269	-0.0272	-0.0829	-0.3838
9	-0.4718	-0.0269	0.0272	0.0829	0.3838
13	0.2718	0.0269	-0.0272	-0.0829	-0.1838
13	-0.0426	-0.0269	0.0272	0.0829	0.1838
17	-0.1574	0.0269	-0.0272	-0.0829	0.0162
17	0.1574	-0.0269	0.0272	0.0829	-0.0162
21	-0.3574	0.0269	-0.0272	-0.0829	0.2162
21	0.2312	-0.0269	0.0272	0.0829	-0.0902
23.387	-0.3505	0.0269	-0.0272	-0.0829	0.2096
23.387	0.0780	-0.0221	0.0103	0.0436	0.0008
25.774	-0.1974	0.0221	-0.0103	-0.0436	0.1185
25.774	-0.0501	-0.0145	-0.0085	-0.0024	0.0550
28.161	-0.0693	0.0145	0.0085	0.0024	0.0643
28.161	-0.1289	-0.0068	-0.0210	-0.0356	0.0790
30.548	0.0096	0.0068	0.0210	0.0356	0.0404
30.548	-0.1571	-0.0007	-0.0248	-0.0496	0.0822
32.936	0.0377	0.0007	0.0248	0.0496	0.0372
32.936	-0.1483	0.0027	-0.0219	-0.0472	0.0747
35.323	0.0290	-0.0027	0.0219	0.0472	0.0446
35.323	-0.1221	0.0039	-0.0155	-0.0354	0.0655

37.71	0.0027	-0.0039	0.0155	0.0354	0.0538
37.71	-0.0960	0.0035	-0.0087	-0.0212	0.0611
40.097	-0.0234	-0.0035	0.0087	0.0212	0.0582
40.097	-0.0819	0.0024	-0.0033	-0.0093	0.0659
42.484	-0.0374	-0.0024	0.0033	0.0093	0.0534
42.484	-0.0856	0.0013	-0.0001	-0.0016	0.0822
44.871	-0.0337	-0.0013	0.0001	0.0016	0.0371
44.871	-0.1060	0.0004	0.0013	0.0021	0.1089
47.258	-0.0134	-0.0004	-0.0013	-0.0021	0.0105
47.258	-0.1316	0.0000	0.0014	0.0030	0.1363
49.645	0.0122	0.0000	-0.0014	-0.0030	-0.0169
49.645	-0.1334	-0.0002	0.0011	0.0024	0.1374
52.032	0.0141	0.0002	-0.0011	-0.0024	-0.0180
52.032	-0.0541	-0.0002	0.0005	0.0013	0.0563
54.419	-0.0652	0.0002	-0.0005	-0.0013	0.0630
54.419	0.1952	-0.0001	0.0001	0.0003	-0.1950
56.807	-0.3146	0.0001	-0.0001	-0.0003	0.3143

Moment values with no scour

Elevation (ft)	Pile 1 Moment (kip-ft)	Pile 2 Moment (kip-ft)	Pile 3 Moment (kip-ft)	Pile 4 Moment (kip-ft)	Pile 5 Moment (kip-ft)
1	4.4339	0.9256	-0.2221	-1.3857	-4.4119
4	-2.4711	-0.7736	0.1671	1.1208	2.6250
4	2.4711	0.7736	-0.1671	-1.1208	-2.6250
7	-0.9594	-0.6215	0.1120	0.8556	1.2892
7	0.9594	0.6215	-0.1120	-0.8556	-1.2892
10	0.1009	-0.4692	0.0569	0.5903	0.4048
10	-0.1009	0.4692	-0.0569	-0.5903	-0.4048
13	0.2896	-0.3169	0.0018	0.3248	-0.0282
13	-0.2896	0.3169	-0.0018	-0.3248	0.0282
16	0.0268	-0.1644	-0.0533	0.0592	-0.0097
16	-0.0401	0.1644	0.0533	-0.0592	0.0231
18.72	-0.2365	-0.0255	-0.1035	-0.1827	0.0323
18.72	0.2365	0.0255	0.1035	0.1827	-0.0323
21.441	-0.2815	0.0686	-0.1219	-0.3153	-0.0392
21.441	0.2815	-0.0686	0.1219	0.3153	0.0392
24.161	-0.2055	0.1058	-0.1078	-0.3245	-0.1152
24.161	0.2055	-0.1058	0.1078	0.3245	0.1152

26.882	-0.1005	0.0986	-0.0755	-0.2521	-0.1448
26.882	0.1005	-0.0986	0.0755	0.2521	0.1448
29.602	-0.0212	0.0691	-0.0412	-0.1530	-0.1260
29.602	0.0212	-0.0691	0.0412	0.1530	0.1260
32.323	0.0145	0.0369	-0.0151	-0.0678	-0.0786
32.323	-0.0145	-0.0369	0.0151	0.0678	0.0786
35.043	0.0132	0.0128	-0.0003	-0.0136	-0.0251
35.043	-0.0132	-0.0128	0.0003	0.0136	0.0251
37.764	-0.0068	-0.0003	0.0053	0.0109	0.0182
37.764	0.0068	0.0003	-0.0053	-0.0109	-0.0182
40.484	-0.0237	-0.0048	0.0054	0.0158	0.0394
40.484	0.0237	0.0048	-0.0054	-0.0158	-0.0394
43.204	-0.0119	-0.0046	0.0035	0.0117	0.0234
43.204	0.0119	0.0046	-0.0035	-0.0117	-0.0234
45.925	0.0578	-0.0028	0.0015	0.0059	-0.0521
45.925	-0.0578	0.0028	-0.0015	-0.0059	0.0521
48.645	0.2071	-0.0011	0.0003	0.0019	-0.2055
48.645	-0.2071	0.0011	-0.0003	-0.0019	0.2055
51.366	0.4053	-0.0002	-0.0001	0.0000	-0.4057
51.366	-0.4053	0.0002	0.0001	0.0000	0.4057
54.086	0.4715	0.0000	-0.0001	-0.0003	-0.4722
54.086	-0.4715	0.0000	0.0001	0.0003	0.4722
56.807	-0.0619	0.0000	0.0000	0.0000	0.0619

Moment values with 5ft scour

Elevation (ft)	Pile 1 Moment (kip-ft)	Pile 2 Moment (kip-ft)	Pile 3 Moment (kip-ft)	Pile 4 Moment (kip-ft)	Pile 5 Moment (kip-ft)
1	5.5029	0.6732	-0.3968	-1.4999	-5.4104
5	-2.4056	-0.5664	0.2880	1.1687	2.6666
5	2.4056	0.5664	-0.2880	-1.1687	-2.6666
9	-0.1103	-0.4594	0.1791	0.8372	0.7247
9	0.1103	0.4594	-0.1791	-0.8372	-0.7247
13	1.3824	-0.3522	0.0701	0.5053	-0.4148
13	-1.3824	0.3522	-0.0701	-0.5053	0.4148
17	1.1518	-0.2450	-0.0390	0.1731	-0.7515
17	-1.1518	0.2450	0.0390	-0.1731	0.7515
21	0.1180	-0.1376	-0.1481	-0.1592	-0.2852
21	-0.2042	0.1376	0.1481	0.1592	0.3713

23.387	-0.4930	-0.0731	-0.2135	-0.3585	-0.0123
23.387	0.4930	0.0731	0.2135	0.3585	0.0123
25.774	-0.8233	-0.0200	-0.2382	-0.4635	0.1287
25.774	0.8233	0.0200	0.2382	0.4635	-0.1287
28.161	-0.8466	0.0148	-0.2179	-0.4580	0.1398
28.161	0.8466	-0.0148	0.2179	0.4580	-0.1398
30.548	-0.6808	0.0311	-0.1676	-0.3727	0.0935
30.548	0.6808	-0.0311	0.1676	0.3727	-0.0935
32.936	-0.4476	0.0329	-0.1081	-0.2536	0.0396
32.936	0.4476	-0.0329	0.1081	0.2536	-0.0396
35.323	-0.2353	0.0263	-0.0556	-0.1402	0.0035
35.323	0.2353	-0.0263	0.0556	0.1402	-0.0035
37.71	-0.0857	0.0170	-0.0185	-0.0551	-0.0106
37.71	0.0857	-0.0170	0.0185	0.0551	0.0106
40.097	0.0012	0.0086	0.0023	-0.0042	-0.0141
40.097	-0.0012	-0.0086	-0.0023	0.0042	0.0141
42.484	0.0545	0.0027	0.0103	0.0182	-0.0291
42.484	-0.0545	-0.0027	-0.0103	-0.0182	0.0291
44.871	0.1166	-0.0004	0.0106	0.0219	-0.0832
44.871	-0.1166	0.0004	-0.0106	-0.0219	0.0832
47.258	0.2275	-0.0015	0.0076	0.0169	-0.2010
47.258	-0.2275	0.0015	-0.0076	-0.0169	0.2010
49.645	0.3997	-0.0014	0.0041	0.0097	-0.3845
49.645	-0.3997	0.0014	-0.0041	-0.0097	0.3845
52.032	0.5763	-0.0008	0.0016	0.0040	-0.5705
52.032	-0.5763	0.0008	-0.0016	-0.0040	0.5705
54.419	0.5630	-0.0003	0.0003	0.0008	-0.5624
54.419	-0.5630	0.0003	-0.0003	-0.0008	0.5624
56.807	-0.0476	0.0000	0.0000	0.0000	0.0476

APPENDIX B

SAMPLE EXTREME LOAD EVENT (1:12) DATA

Shear values with no scour

Elevation (ft)	Pile 1 Shear (kips)	Pile 2 Shear (kips)	Pile 3 Shear (kips)	Pile 4 Shear (kips)	Pile 5 Shear (kips)
1	36.5510	38.0560	37.8090	37.8820	37.4030
4	-36.7010	-38.0560	-37.8090	-37.8820	-37.2530
4	36.8360	37.8670	37.6850	37.7630	37.4370
7	-36.9860	-37.8670	-37.6850	-37.7630	-37.2870
7	36.8820	37.8530	37.6190	37.7260	37.2830
10	-37.0320	-37.8530	-37.6190	-37.7260	-37.1330
10	37.0360	37.8580	37.6220	37.7290	37.1330
13	-37.1860	-37.8580	-37.6220	-37.7290	-36.9830
13	37.1840	37.8540	37.6190	37.7270	36.9830
16	-37.3340	-37.8540	-37.6190	-37.7270	-36.8330
16	37.1740	37.8390	37.6040	37.7090	36.9510
18.72	-37.3100	-37.8390	-37.6040	-37.7090	-36.8150
18.72	27.0610	27.5820	27.3760	27.4860	27.0420
21.441	-27.1970	-27.5820	-27.3760	-27.4860	-26.9060
21.441	9.8035	10.0010	9.8539	9.9616	9.9362
24.161	-9.9395	-10.0010	-9.8539	-9.9616	-9.8002
24.161	-7.3398	-7.4696	-7.5406	-7.4486	-7.0916
26.882	7.2038	7.4696	7.5406	7.4486	7.2276
26.882	-18.9960	-19.4080	-19.4070	-19.3520	-18.6320
29.602	18.8600	19.4080	19.4070	19.3520	18.7680
29.602	-26.6250	-27.1230	-27.0730	-27.0800	-26.1280
32.323	26.4890	27.1230	27.0730	27.0800	26.2640
32.323	-25.4380	-25.2990	-25.2330	-25.3590	-24.8640
35.043	25.3020	25.2990	25.2330	25.3590	25.0000
35.043	-17.0520	-16.6140	-16.5670	-16.7060	-16.5670
37.764	16.9160	16.6140	16.5670	16.7060	16.7030
37.764	-8.1886	-7.7326	-7.7088	-7.8067	-7.8458
40.484	8.0526	7.7326	7.7088	7.8067	7.9818
40.484	-2.0895	-1.7569	-1.7502	-1.7991	-1.8458

43.204	1.9535	1.7569	1.7502	1.7991	1.9818
43.204	0.8058	0.9938	0.9920	0.9781	1.0333
45.925	-0.9418	-0.9938	-0.9920	-0.9781	-0.8973
45.925	1.4587	1.5441	1.5400	1.5434	1.7410
48.645	-1.5947	-1.5441	-1.5400	-1.5434	-1.6049
48.645	1.0597	1.0961	1.0930	1.1008	1.3926
51.366	-1.1957	-1.0961	-1.0930	-1.1008	-1.2566
51.366	0.4433	0.4709	0.4694	0.4755	0.6415
54.086	-0.5793	-0.4709	-0.4694	-0.4755	-0.5055
54.086	0.0033	0.0486	0.0484	0.0505	-0.4423
56.807	-0.1393	-0.0486	-0.0484	-0.0505	0.5783

Shear values with 5ft of scour

Elevation (ft)	Pile 1 Shear (kips)	Pile 2 Shear (kips)	Pile 3 Shear (kips)	Pile 4 Shear (kips)	Pile 5 Shear (kips)
1	35.321	37.653	36.996	36.564	37.738
5	-35.521	-37.653	-36.996	-36.564	-37.538
5	35.52	37.672	36.975	36.568	37.629
9	-35.72	-37.672	-36.975	-36.568	-37.429
9	35.713	37.596	36.901	36.553	37.42
13	-35.913	-37.596	-36.901	-36.553	-37.22
13	35.913	37.601	36.902	36.553	37.222
17	-36.113	-37.601	-36.902	-36.553	-37.022
17	36.111	37.593	36.898	36.552	37.02
21	-36.311	-37.593	-36.898	-36.552	-36.82
21	36.174	37.587	36.891	36.542	36.948
23.387	-36.293	-37.587	-36.891	-36.542	-36.828
23.387	27.971	29.206	28.551	28.23	28.919
25.774	-28.09	-29.206	-28.551	-28.23	-28.8
25.774	13.025	13.775	13.198	12.999	13.952
28.161	-13.145	-13.775	-13.198	-12.999	-13.833
28.161	-3.9989	-3.8523	-4.2279	-4.3696	-3.279
30.548	3.8795	3.8523	4.2279	4.3696	3.3983
30.548	-17.992	-18.606	-18.704	-18.621	-17.719
32.936	17.873	18.606	18.704	18.621	17.839
32.936	-28.41	-29.65	-29.494	-29.286	-28.565
35.323	28.291	29.65	29.494	29.286	28.685
35.323	-34.846	-36.429	-36.042	-35.703	-35.41

37.71	34.727	36.429	36.042	35.703	35.53
37.71	-31.863	-32.698	-32.183	-31.819	-32.75
40.097	31.744	32.698	32.183	31.819	32.87
40.097	-22.772	-23.283	-22.83	-22.524	-23.469
42.484	22.653	23.283	22.83	22.524	23.588
42.484	-12.42	-12.403	-12.123	-11.947	-12.741
44.871	12.3	12.403	12.123	11.947	12.86
44.871	-4.5004	-4.2433	-4.1171	-4.0473	-4.4376
47.258	4.381	4.2433	4.1171	4.0473	4.557
47.258	0.14101	0.42926	0.45261	0.45706	0.49786
49.645	-0.26036	-0.42926	-0.45261	-0.45706	-0.37851
49.645	2.0198	2.2354	2.2083	2.1839	2.478
52.032	-2.1391	-2.2354	-2.2083	-2.1839	-2.3586
52.032	2.0569	2.1805	2.1426	2.1152	2.2418
54.419	-2.1762	-2.1805	-2.1426	-2.1152	-2.1225
54.419	0.94571	1.008	0.98747	0.97381	0.18124
56.807	-1.0651	-1.008	-0.98747	-0.97381	-0.06189

Moment values with no scour

Elevation (ft)	Pile 1 Moment (kip-ft)	Pile 2 Moment (kip-ft)	Pile 3 Moment (kip-ft)	Pile 4 Moment (kip-ft)	Pile 5 Moment (kip-ft)
1	-477.2	-502.57	-494.69	-493.19	-498.28
4	367.17	388.22	381.2	379.6	385.59
4	-367.82	-388.86	-381.91	-380.16	-385.55
7	257.25	274.77	268.66	267	272.27
7	-257.33	-274.78	-268.71	-267.03	-272.28
10	146.77	160.53	155.57	154.01	159.14
10	-146.76	-160.53	-155.57	-154.01	-159.14
13	35.796	46.139	42.363	40.982	46.266
13	-35.798	-46.14	-42.365	-40.984	-46.263
16	-75.61	-68.296	-70.875	-72.058	-66.238
16	75.6	68.29	70.87	72.058	66.243
18.72	-176.61	-172.46	-173.99	-175.02	-168.14
18.72	176.61	172.46	173.99	175.03	168.13
21.441	-250.11	-248.46	-249.08	-250.07	-242.78
21.441	250.11	248.46	249.08	250.07	242.78
24.161	-276.65	-276.24	-276.21	-277.24	-270.48
24.161	276.65	276.24	276.21	277.24	270.48

26.882	-256.53	-256.11	-255.73	-256.84	-251.42
26.882	256.53	256.11	255.73	256.84	251.42
29.602	-204.71	-203.22	-202.75	-203.92	-200.64
29.602	204.71	203.22	202.75	203.92	200.64
32.323	-132.15	-129.15	-128.79	-129.89	-129.25
32.323	132.15	129.15	128.79	129.9	129.25
35.043	-62.877	-60.017	-59.824	-60.579	-61.221
35.043	62.877	60.016	59.824	60.578	61.22
37.764	-16.513	-14.602	-14.539	-14.916	-15.805
37.764	16.513	14.602	14.539	14.916	15.805
40.484	5.6489	6.5414	6.5352	6.4217	5.8106
40.484	-5.6489	-6.5414	-6.5352	-6.4217	-5.8106
43.204	11.163	11.349	11.322	11.339	11.044
43.204	-11.163	-11.349	-11.322	-11.339	-11.044
45.925	8.7754	8.6357	8.6116	8.6652	8.4144
45.925	-8.7754	-8.6357	-8.6116	-8.6652	-8.4144
48.645	4.6071	4.4163	4.4029	4.4466	3.8493
48.645	-4.6071	-4.4163	-4.4029	-4.4466	-3.8493
51.366	1.5286	1.4203	1.4155	1.4377	0.23388
51.366	-1.5286	-1.4203	-1.4155	-1.4377	-0.23388
54.086	0.13276	0.13296	0.1323	0.13807	-1.3314
54.086	-0.13276	-0.13296	-0.1323	-0.13807	1.3314
56.807	-0.06188	0	0	0	0.061884

Moment values with 5ft of scour

Elevation (ft)	Pile 1 Moment (kip-ft)	Pile 2 Moment (kip-ft)	Pile 3 Moment (kip-ft)	Pile 4 Moment (kip-ft)	Pile 5 Moment (kip-ft)
1	-529.95	-585.92	-561.98	-545.92	-591.36
5	388.49	434.68	413.8	400.01	439.38
5	-388.67	-435.42	-414.52	-400.23	-439.42
9	247.38	283.12	266.12	254.77	286.47
9	-247.39	-283.2	-266.2	-254.79	-286.48
13	105.65	130.66	117.91	109.52	133.6
13	-105.64	-130.66	-117.9	-109.51	-133.6
17	-36.826	-22.17	-30.518	-35.754	-18.866
17	36.827	22.171	30.522	35.755	18.86
21	-180.21	-175	-178.98	-181.11	-170.54
21	180.12	175.01	178.98	181.11	170.63

23.387	-265.85	-266.54	-268	-268.37	-260.9
23.387	265.86	266.54	268	268.38	260.9
25.774	-332.08	-337.72	-336.91	-335.77	-331.66
25.774	332.01	337.71	336.95	335.69	331.64
28.161	-362.63	-371.6	-368.92	-366.62	-366.18
28.161	362.63	371.54	368.94	366.62	366.18
30.548	-352.7	-362.87	-358.99	-355.95	-359.09
30.548	352.68	362.85	359.05	355.94	359.08
32.936	-309.43	-318.56	-314.29	-311.13	-317.06
32.936	309.41	318.57	314.3	311.12	317.06
35.323	-241.34	-247.61	-243.58	-240.77	-248.8
35.323	241.34	247.61	243.58	240.77	248.8
37.71	-157.94	-160.27	-157.11	-155.06	-163.98
37.71	157.94	160.27	157.11	155.06	163.98
40.097	-81.737	-81.815	-79.881	-78.685	-85.434
40.097	81.736	81.816	79.88	78.685	85.437
42.484	-27.333	-25.934	-25.088	-24.628	-29.076
42.484	27.333	25.934	25.088	24.628	29.076
44.871	2.2665	3.8445	4.0098	4.0426	1.6022
44.871	-2.2665	-3.8445	-4.0098	-4.0426	-1.6022
47.258	12.898	14.038	13.894	13.754	12.389
47.258	-12.898	-14.038	-13.894	-13.754	-12.389
49.645	12.414	13.013	12.81	12.656	11.349
49.645	-12.414	-13.013	-12.81	-12.656	-11.349
52.032	7.4311	7.6508	7.5115	7.4139	5.5609
52.032	-7.4311	-7.6508	-7.5115	-7.4139	-5.5609
54.419	2.3607	2.4187	2.3697	2.3372	0.33677
54.419	-2.3607	-2.4187	-2.3697	-2.3372	-0.33677
56.807	-0.04765	0	0	0	0.047648

APPENDIX C

SAMPLE EXTREME LOAD EVENT (1:4) DATA

Shear values with no scour

Elevation (ft)	Pile 1 Shear (kips)	Pile 2 Shear (kips)	Pile 3 Shear (kips)	Pile 4 Shear (kips)	Pile 5 Shear (kips)
1	28.974	31.173	30.4	31.062	31.487
4	-29.424	-31.173	-30.4	-31.062	-31.037
4	29.891	31.382	30.613	31.583	31.272
7	-30.341	-31.382	-30.613	-31.583	-30.822
7	30.322	31.383	30.613	31.553	30.823
10	-30.772	-31.383	-30.613	-31.553	-30.373
10	30.768	31.38	30.609	31.552	30.371
13	-31.218	-31.38	-30.609	-31.552	-29.921
13	31.218	31.382	30.612	31.548	29.922
16	-31.668	-31.382	-30.612	-31.548	-29.472
16	30.619	31.371	30.603	31.536	29.262
18.622	-31.012	-31.371	-30.603	-31.536	-28.868
18.622	21.41	22.177	21.499	22.382	20.799
21.244	-21.803	-22.177	-21.499	-22.382	-20.406
21.244	6.9329	6.7449	6.2513	6.9916	6.9413
23.866	-7.3262	-6.7449	-6.2513	-6.9916	-6.548
23.866	-6.8271	-7.8011	-8.0563	-7.5545	-6.3042
26.487	6.4338	7.8011	8.0563	7.5545	6.6975
26.487	-14.987	-16.727	-16.761	-16.562	-14.033
29.109	14.594	16.727	16.761	16.562	14.426
29.109	-19.841	-21.629	-21.461	-21.659	-18.564
31.731	19.448	21.629	21.461	21.659	18.957
31.731	-18.911	-18.21	-17.943	-18.496	-17.727
34.353	18.517	18.21	17.943	18.496	18.121
34.353	-12.977	-11.106	-10.877	-11.402	-12.086
36.975	12.583	11.106	10.877	11.402	12.479
36.975	-6.5844	-4.663	-4.5271	-4.8683	-5.9321
39.597	6.1911	4.663	4.5271	4.8683	6.3254
39.597	-2.0307	-0.65844	-0.60466	-0.7591	-1.4531

42.219	1.6374	0.65844	0.60466	0.7591	1.8464
42.219	0.27229	0.99469	0.99962	0.96753	0.97718
44.841	-0.66557	-0.99469	-0.99962	-0.96753	-0.5839
44.841	0.91675	1.1712	1.1576	1.1795	1.8908
47.462	-1.31	-1.1712	-1.1576	-1.1795	-1.4975
47.462	0.71757	0.7497	0.73538	0.76664	1.8553
50.084	-1.1108	-0.7497	-0.73538	-0.76664	-1.462
50.084	0.28337	0.28274	0.27438	0.29537	0.8792
52.706	-0.67665	-0.28274	-0.27438	-0.29537	-0.48592
52.706	-0.08503	0.006652	0.004526	0.011026	-1.806
55.328	-0.30825	-0.00665	-0.00453	-0.01103	2.1992

Shear values with 5ft of scour

Elevation (ft)	Pile 1 Shear (kips)	Pile 2 Shear (kips)	Pile 3 Shear (kips)	Pile 4 Shear (kips)	Pile 5 Shear (kips)
1	26.881	29.199	28.354	29.556	30.021
5	-27.481	-29.199	-28.354	-29.556	-29.421
5	27.295	29.397	28.585	29.247	29.636
9	-27.895	-29.397	-28.585	-29.247	-29.036
9	27.797	29.396	28.583	29.236	29.035
13	-28.397	-29.396	-28.583	-29.236	-28.435
13	28.395	29.398	28.586	29.227	28.439
17	-28.995	-29.398	-28.586	-29.227	-27.839
17	28.995	29.391	28.583	29.227	27.83
21	-29.595	-29.391	-28.583	-29.227	-27.23
21	28.683	29.389	28.578	29.215	27.133
23.289	-29.026	-29.389	-28.578	-29.215	-26.79
23.289	21.518	22.146	21.421	22.043	20.72
25.577	-21.861	-22.146	-21.421	-22.043	-20.377
25.577	9.5591	9.0975	8.5519	9.1099	9.3647
27.866	-9.9024	-9.0975	-8.5519	-9.1099	-9.0214
27.866	-3.6149	-5.2418	-5.5489	-5.1056	-3.3329
30.154	3.2716	5.2418	5.5489	5.1056	3.6761
30.154	-13.915	-15.977	-16.028	-15.759	-13.252
32.443	13.571	15.977	16.028	15.759	13.595
32.443	-20.428	-23.085	-22.919	-22.876	-19.441
34.731	20.085	23.085	22.919	22.876	19.784
34.731	-24.06	-26.116	-25.697	-26.079	-22.818

37.02	23.717	26.116	25.697	26.079	23.162
37.02	-22.304	-21.183	-20.804	-21.383	-21.087
39.308	21.961	21.183	20.804	21.383	21.43
39.308	-16.165	-13.493	-13.223	-13.744	-15.047
41.597	15.822	13.493	13.223	13.744	15.391
41.597	-9.3102	-6.4611	-6.3155	-6.67	-8.2011
43.885	8.9669	6.4611	6.3155	6.67	8.5443
43.885	-3.831	-1.639	-1.5883	-1.7704	-2.5836
46.174	3.4878	1.639	1.5883	1.7704	2.9269
46.174	-0.40794	0.85409	0.84978	0.79472	1.0242
48.462	0.064657	-0.85409	-0.84978	-0.79472	-0.68089
48.462	1.1573	1.6158	1.5898	1.6054	2.4663
50.751	-1.5006	-1.6158	-1.5898	-1.6054	-2.123
50.751	1.3685	1.3597	1.3341	1.3723	1.5374
53.039	-1.7118	-1.3597	-1.3341	-1.3723	-1.1941
53.039	0.6217	0.57082	0.55888	0.58269	-2.4423
55.328	-0.96498	-0.57082	-0.55888	-0.58269	2.7856

Moment values with no scour

Elevation (ft)	Pile 1 Moment (kip-ft)	Pile 2 Moment (kip-ft)	Pile 3 Moment (kip-ft)	Pile 4 Moment (kip-ft)	Pile 5 Moment (kip-ft)
1	-416.76	-429	-409.22	-421.68	-430.88
4	326.57	335.36	317.98	328.57	334.1
4	-326.67	-335.23	-317.85	-328.67	-333.96
7	233.98	240.59	225.88	234.23	237.36
7	-234	-240.59	-225.88	-234.27	-237.36
10	140.17	145.65	133.84	140.05	141.79
10	-140.16	-145.65	-133.84	-140.05	-141.79
13	45.058	50.548	41.751	45.903	47.412
13	-45.058	-50.555	-41.749	-45.906	-47.417
16	-51.421	-44.626	-50.375	-48.223	-45.658
16	51.366	44.625	50.374	48.223	45.715
18.622	-134	-131.26	-134.27	-133.99	-125.33
18.622	133.99	131.25	134.27	133.99	125.32
21.244	-191.81	-192.59	-193.24	-194.83	-181.91
21.244	191.81	192.59	193.23	194.83	181.91
23.866	-210.65	-211.54	-210.47	-213.69	-200.82
23.866	210.65	211.54	210.47	213.69	200.82

26.487	-192.45	-190.54	-188.54	-192.89	-183.69
26.487	192.45	190.53	188.54	192.89	183.69
29.109	-152.33	-144.99	-142.77	-147.54	-145.47
29.109	152.32	144.98	142.77	147.53	145.48
31.731	-99.167	-85.924	-84.132	-88.301	-94.883
31.731	99.169	85.929	84.135	88.298	94.889
34.353	-48.574	-36.17	-35.095	-37.736	-46.479
34.353	48.574	36.167	35.095	37.736	46.471
36.975	-14.037	-5.8048	-5.3639	-6.5721	-13.275
36.975	14.037	5.8048	5.3639	6.5721	13.275
39.597	3.2206	6.9504	7.0129	6.7308	3.2985
39.597	-3.2206	-6.9504	-7.0129	-6.7308	-3.2985
42.219	8.1723	8.7567	8.6677	8.803	7.7662
42.219	-8.1723	-8.7567	-8.6677	-8.803	-7.7662
44.841	6.9024	6.041	5.9363	6.1573	5.6619
44.841	-6.9024	-6.041	-5.9363	-6.1573	-5.6619
47.462	3.8925	2.8406	2.7725	2.9329	1.0859
47.462	-3.8925	-2.8406	-2.7725	-2.9329	-1.0859
50.084	1.4217	0.79139	0.76247	0.83743	-3.3949
50.084	-1.4217	-0.79139	-0.76247	-0.83743	3.3949
52.706	0.12447	0.018359	0.012438	0.030122	-5.2374
52.706	-0.12447	-0.01836	-0.01244	-0.03012	5.2374
55.328	-0.17714	0	0	0	0.17714
min	-416.76	-429	-409.22	-421.68	-430.88
max	326.57	335.36	317.98	328.57	334.1
sum	-417.12	-428.906	-409.096	-421.836	-430.513

Moment values with 5ft of scour

Elevation (ft)	Pile 1 Moment (kip-ft)	Pile 2 Moment (kip-ft)	Pile 3 Moment (kip-ft)	Pile 4 Moment (kip-ft)	Pile 5 Moment (kip-ft)
1	-454.66	-484.44	-455.49	-459.66	-491.8
5	342.84	367.35	341.99	341.71	369.02
5	-344.32	-367.48	-342.07	-343.05	-369.15
9	231.66	248.54	227.44	227.08	246.75
9	-231.78	-248.54	-227.44	-227.12	-246.75
13	117.48	128.91	112.67	111.56	126.03
13	-117.47	-128.91	-112.66	-111.56	-126.03
17	0.88654	8.8892	-2.2244	-3.8247	7.3511

17	-0.88653	-8.8848	2.2242	3.8248	-7.3497
21	-118.22	-111.18	-117.14	-119.26	-108.89
21	117.94	111.18	117.13	119.26	109.17
23.289	-185.1	-183.06	-186.04	-188.61	-174.23
23.289	185.1	183.06	186.04	188.61	174.23
25.577	-235.47	-237.31	-237.71	-240.89	-223.97
25.577	235.47	237.31	237.71	240.89	223.97
27.866	-257.79	-259.97	-258.43	-262.29	-246.64
27.866	257.79	259.97	258.43	262.29	246.64
30.154	-249.23	-247.96	-245.24	-249.73	-239.07
30.154	249.23	247.96	245.24	249.73	239.07
32.443	-216.53	-209.96	-206.86	-211.72	-207.85
32.443	216.53	209.96	206.86	211.72	207.85
34.731	-168.6	-154.73	-151.9	-156.73	-161.83
34.731	168.6	154.73	151.89	156.73	161.83
37.02	-112.18	-92.126	-90.238	-94.1	-107.71
37.02	112.18	92.13	90.241	94.1	107.7
39.308	-59.954	-41.305	-40.315	-42.774	-57.591
39.308	59.954	41.301	40.315	42.774	57.589
41.597	-22.225	-8.9102	-8.5788	-9.792	-21.689
41.597	22.225	8.9102	8.5788	9.792	21.689
43.885	-0.67381	6.6092	6.5816	6.2104	-1.9264
43.885	0.67381	-6.6092	-6.5816	-6.2104	1.9264
46.174	7.9529	10.552	10.396	10.455	4.5851
46.174	-7.9529	-10.552	-10.396	-10.455	-4.5851
48.462	8.5068	8.5078	8.3579	8.5458	2.5833
48.462	-8.5068	-8.5078	-8.3579	-8.5458	-2.5833
50.751	5.3704	4.6322	4.5429	4.6922	-2.8223
50.751	-5.3704	-4.6322	-4.5429	-4.6922	2.8223
53.039	1.7366	1.3696	1.3412	1.3985	-6.0373
53.039	-1.7366	-1.3696	-1.3412	-1.3985	6.0373
55.328	-0.13496	0	0	0	0.13496

REFERENCES

AASHTO. (2010). "LRFD Bridge Specifications."

AASHTO. (2009). "Vessel Collision Design of Highway Bridges."

AASHTO, S., J. D. (1997a). *Instrumentation for measuring scour at bridge piers and abutments*, American Association of State Highway and Transportation Officials National Academy Press, Washington, D.C.

AASHTO, S., J. D. (1997b). *Magnetic sliding collar scour monitor : installation, operation, and fabrication manual*, American Association of State Highway and Transportation Officials National Academy Press, Transportation Research Board, National Research Council, Washington, D.C.

AASHTO, S., J. D. (1997c). *Sonar scour monitor : installation, operation, and fabrication manual*, American Association of State Highway and Transportation Officials National Academy Press, Washington, D.C.

Anderson, J. B., Townsend, F. C., and Grajales, B. (2003). "Case History Evaluation of Laterally Loaded Piles." *Journal of Geotechnical & Geoenvironmental Engineering*, 129(3), 187.

Bennett, C. (2010). "Scour effects on the response of laterally loaded piles considering stress history of sand." 37(Issues 7–8), 1008–1014.

Bennett, C. "A Literature Review on Behavior of Scoured Piles under Bridges." *ASCE Conference Proceedings*, 62-62.

Bennett, C., Han, J., and Parsons, R. L. (2012). "Integrated Analysis of the Performance of Pile-supported Bridges under Scoured Conditions." *Engineering structures*, 36, 27-38.

Bui, L. H. (2005). "Static Versus Dynamic Structural Response of Bridge Piers to Barge Collision Loads," University of Florida.

Chen, Y. (1997). "Assessment of Pile Effective Lengths and Their Effects on Design." Computers and Structures, 265-286.

Consolazio, G. R. (2009). "A Static Analysis Method for Barge-Impact Design of Bridges with Consideration of Dynamic Amplifcation." Florida Department of Transportation, University of Florida, USA.

Coskun, F. (1995). "Hydrological Aspects of Bridge Design: Case Study." *Journal of irrigation and drainage engineering*, 121(6), 411-418.

Deng, L., and Cai, C. S. (2010). "Bridge Scour: Prediction, Modeling, Monitoring, and Countermeasures—Review." *Practice Periodical on Structural Design & Construction*, 15(2), 125-134.

Ellis, C. (2008). "Ernest F. Lyons Bridge Replacement Project Brochure." ASPIRE.

FDOT. (2013). "FDOT - Roadway Design Office."

FHWA. (2012). "Evaluating Scour at Bridges." HEC-18, FHWA.

Institute, F. B. S. (2000). "FB-MultiPier Manual." University of Florida, USA.

Kim, J. B. (1984). "Pile Caps Subjected to Lateral Loads." ASCE National Convention, San Francisco, C.A.

Lagasse, P. F. (2013). "Countermeasures to Protect Bridge Piers from Scour | Blurbs | Publications."

Liang, F. "A Literature Review on Behavior of Scoured Piles under Bridges." *ASCE Conference Proceedings*, 62-62.

Lin, C., Bennett, C., Han, J., and Parsons, R. L. "p - y Based Approach for Buckling Analysis of Axially Loaded Piles under Scoured Conditions." *ASCE Conference Proceedings*, 12-12.

McCann, D. M., Clark, M. R., Broughton, K. J., and Fenning, P. J. (1999). "Radar measurement of bridge scour." *NDT & E international : independent nondestructive testing and evaluation*, 32(8), 481-492.

McVay, M. C., Wasman, S. J., Consolazio, G. R., Bullock, P. J., Cowan, D. G., and Bollmann, H. T. (2012). "Dynamic Soil–Structure Interaction of Bridge Substructure Subject to Vessel Impact."

Mele, R. (2002). "The monitoring of bridges for scour by sonar and sedimetri." *NDT & E international : independent nondestructive testing and evaluation*, 35(2), 117-123.

Nowak, A., and Knott, M. "Extreme Load Events and their Combinations." *The Design of Bridges for Extreme Events*, Atlanta, GA.

Paduana, J. A., and Yee, W. S. (1974). "Lateral Load Tests on Piles in Bridge Embankment." Transportation Research Board, Washington, D.C., 77-92.

Poulos, H. G., and Davis, E. H. (1980). "Pile Foundations Analysis And Design." John Wiley & Sons, New York, N.Y.

Puleo, J. A. (2011). "Near Real-Time Scour Monitoring System: Application to Indian River Inlet, Delaware." *Journal of hydraulic engineering (New York, N.Y.)*, 137(9), 1037-1046.

Reese, L. C., Cox, W. R., and Koop, F. D. (1974). "Analysis of Lateraly Loaded Piles in Sand." Fifth Annual Offshore Technology Conference, Houston, Texas.

Robinson, B., Suarez, V., Gabr, M. A., and Kowalsky, M. (2011). "Simplified Lateral Analysis of Deep Foundation Supported Bridge Bents: Driven Pile Case Studies."

Rollins, K. M., and Stenlund, T. E. (2010). "Laterally Loaded Pile Cap Connections." Utah Department of Transportation Research Division, Brigham Young University.

Sabia, D. (2011). "Influence of Foundation Scour on the Dynamic Response of an Existing Bridge." *Journal of bridge engineering*, 16(2), 295-304.

Sheppard, D. M. (2003). "Large scale and live bed local pier scour experiments.", University of Florida, FDOT Research Center.

Shin, J. H. (2010). "Development and application of a 3-dimensional scour monitoring system for sea-crossing bridge piers." *International Journal of Offshore and Polar Engineering*, 20(4), 292-297.

Unger, J., and Hager, W. H. (2006). "Riprap Failure at Circular Bridge Piers." *Journal of Hydraulic Engineering*, 132(4), 354.

Wang, C., and Kallaka, T. (2011). "Efficient Numerical Model for Studying bridge Pier Collapse in Floods." *World Academy of Science, Engineering, and Technology*, 60, 6.

BIOGRAPHICAL SKETCH

Kakit Fung earned his dual degree of Bachelor of Science in Civil & Environmental Engineering from Florida State University in April 2011. He continued his education in the following fall and will graduate in April 2013 with a Master of Science in Civil Engineering (MSCE).